Transport Effects in Semi-metals and Narrow-gap Semiconductors

By H. J. GOLDSMID

Department of Physics, Bristol College of Science and Technology, Ashley Down, Bristol, 7

ABSTRACT

The semi-metals and narrow-gap semiconductors are characterized by high values of the electron mobility, and sometimes, of the hole mobility too. When both carriers have a high mobility in intrinsic material the bipolar transport effects become prominent. Properties that are particularly sensitive to bipolar conduction are the electronic thermal conductivity and the Nernst and Ettingshausen coefficients.

When there is a very large magnetoresistance effect, as there is in some semi-metals at low temperatures, high electric fields can be applied without excessive power dissipation. This allows the observation of an enhanced phonon interaction with carriers that are drifting with the speed of sound, the effect being manifested as a kink in the current-voltage characteristic. Other non-linear effects have been observed at high current densities due to self-magnetic fields of the charge carriers. These and other effects can be influenced by diffusion phenomena associated with the relatively high carrier lifetimes.

The long relaxation times of the carriers in some of the materials at very low temperatures allow one to observe oscillations in the magnetoresistance (and other properties) as well as size-dependent effects.

Most of the materials have multi-valley energy bands for at least one type of charge carrier. Although the band parameters are given most directly by cyclotron resonance experiments, they can in general also be determined from galvanomagnetic measurements under less critical experimental conditions. Several of the materials belong to the crystal class R3m and have ellipsoidal (or quasi-ellipsoidal) energy surfaces in the Brillouin zone which are tilted with respect to the crystal axes. These materials provide an interesting example of the determination of band structures from the galvanomagnetic coefficients. Even for a two-band non-parabolic conductor, there are generally sufficient data to allow the band parameters for any specific model to be calculated, provided, of course, that the model is appropriate.

Thermoelectric measurements, together with Nernst or magnetothermoelectric observations, can provide the data on the Fermi energy and scattering law that are needed to complete a description of the material.

The high carrier concentrations in the semi-metals (and the heavily-doped semiconductors) give rise to the possibility of superconducting behaviour. In this case, however, a low mobility is an advantage, since a high mobility implies a weak interaction between the electrons and the lattice.

The recent observations on the variation with voltage of the tunnelling current at a junction between a semi-metal and an insulator indicate a promising technique for band-structure studies.

Applications of the semi-metals are somewhat restricted by the parameters of the presently available materials, but the possibility of thermomagnetic energy conversion should encourage comprehensive studies of the transport properties on existing and new semi-metals.

CONTENTS

§Ι.	Introduction.	274
§ 2.	Characteristics of Specific Materials. 2.1. Crystal Structures. 2.2. Electronic Parameters.	277275
§ 3.	TRANSPORT PHENOMENA IN THE ABSENCE OF A MAGNETIC FIELD. 3.1. Thermoelectric Effects and Heat Conduction. 3.2. Size Effect on the Electrical Conductivity.	291 291 296
§ 4.	GALVANOMAGNETIC EFFECTS. 4.1. Determination of the Effective Mass Tensor. 4.2. Oscillatory Magnetoresistance.	298 298 308
§ 5.	Non-Linear Effects. 5.1. Self-magnetic Field and Diffusion Effects. 5.2. Esaki Kink Effect.	305 305 307
§ 6.	THERMOMAGNETIC EFFECTS. 6.1. Nernst and Ettingshausen Effects. 6.2. Magneto-thermal Resistance. 6.3. Magneto-Seebeck Effect. 6.4. Righi-Leduc Effect.	310 310 313 314 318
§ 7.	TUNNEL EFFECT.	318
§ 8.	SUPERCONDUCTIVITY.	319
§ 9.	Applications.	321
Ref	TERENCES.	323

§ 1. Introduction

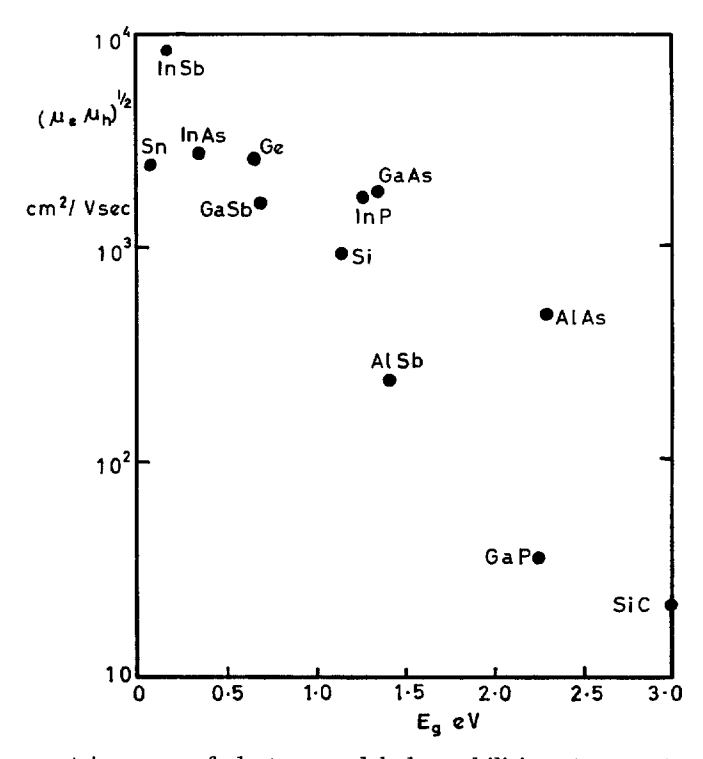
The intensive study of semiconductors in recent years has, for the most part, been concentrated on materials with energy gaps of the order of one or more electron-volts, since it is these substances that can be used in junction devices such as transistors. However, for some types of application it is desirable to choose semiconductors having much smaller energy gaps. This is immediately obvious, for example, if one wishes to develop a photoconductor for long-wavelength infra-red radiation, since the response falls off sharply when the photon energy becomes less than the energy-gap width. It is not so obvious that narrow-gap semiconductors are needed for, say, galvanomagnetic devices until one recollects that, in general, the charge-carrier mobility increases as the energy gap decreases (Wright 1959). This trend is shown in fig. 1 for the Group IV elements and III-V compounds.

If one wishes to study those effects that depend on high carrier mobilities one does not, then, normally work with wide-gap semiconductors. In fact, there is apparently some advantage from this viewpoint if the energy gap disappears altogether; in other words, one should employ a semi-metal rather than a semiconductor.

Before going further we should, perhaps, consider the physical differences between semiconductors and semi-metals. One can define a semiconductor as a material in which there is a band of forbidden energy covering all values of the wavevector. Semi-metals, on the other hand, have no such forbidden band, though they can still retain a direct energy gap for any specific wavevector. It might be expected that these simple definitions

would make it easy to decide if any given material is a semiconductor or a semi-metal but, in practice, this is not always so. A perfectly pure semiconductor should have zero electrical conductivity at the absolute zero of temperature, whereas a semi-metal must retain a finite conductivity However, the donor or acceptor impurities, that are always present in any real semiconductor, invariably have very small activation energies when the gap is narrow, and, unless their concentration is very small, there is a tendency for them to form impurity bands which overlap the conduction or valence bands. This implies that, however low the temperature, the charge carriers are not frozen into the impurity states and the electrical conductivity does not disappear. Also, it must be realized, that even when the valence and conduction bands overlap one another, this does not imply that the carrier concentration must be independent of temperature. For example, consider the simple case of an intrinsic conductor with a parabolic density-of-states function and a density-ofstates effective mass m^* which has the same value for electrons and holes. Then the carrier concentration n_i is given by:

$$n_i = 2 \left(\frac{2\pi m^* kT}{h^2}\right)^{3/2} F_{1/2} \left(\frac{E_g}{2kT}\right), \quad (1)$$



Plot of geometric mean of electron and hole mobilities at room temperature against energy gap for Group IV elements and III-V compounds.

A.P.

where k is Boltzmann's constant, T is the absolute temperature, h is Planck's constant, E_g is the energy gap:

$$F_r(x) = \int_0^\infty x^r f dx,$$

f being the Fermi distribution function. Clearly, even when the energy gap is equal to zero, the carrier concentration varies as $T^{3/2}$, although the temperature variation of the mobility might prevent the electrical conductivity from increasing with temperature.

Semi-metals can be doped with impurities so that they become n- or p-type in just the same way as semiconductors. Furthermore, there are solid-solution systems for which some compositions are semiconducting while others are semi-metallic. For example, Jain (1959) showed that the Bi-Sb alloys are semiconductors over a certain range of composition, whereas both the elements are semi-metals. Since, then, there is so little practical difference between semi-metals and narrow-gap semiconductors it seems appropriate that both types of material should be included in this review.

It is not intended to make an exhaustive coverage of all the materials or phenomena that could legitimately be included. It has already been pointed out that semi-metals and narrow-gap semiconductors tend to have high carrier mobilities. As the temperature is reduced the mobility rises, in many instances to extremely large values which are limited only by crystalline imperfections. In wide-gap semiconductors the low-temperature mobility tends to be restricted by ionized-impurity scattering but in many of the narrow-gap materials this does not occur. This is due, to some extent at least, to the fact that the latter materials generally have large values of the dielectric constant, thereby reducing the range of influence of the impurity ions (Conwell and Weisskopf 1950, Brooks 1955). Also, there is a screening effect at large carrier concentrations. Particular attention, then, will be paid to those materials which exhibit exceptionally high mobilities at low temperatures.

One reason for the study of semi-metals and narrow-gap semiconductors lies in the fact that they can have high concentrations of electrons and holes present simultaneously. Thus, they permit the easy observation of the bipolar transport effects, in which there is appreciable energy transfer without the flow of electronic current. The bipolar effects are seen to most advantage in materials that have high mobilities for both electrons and holes.

Naturally enough, the semi-metal bismuth takes pride of place in this review, since so much effort has been devoted to its study (Boyle and Smith 1963). The elements antimony and, to a lesser extent, arsenic from the same group of the periodic table must also be mentioned in some detail, if only for the purposes of comparison.

There are two other interesting elemental materials, graphite and grey tin, which would certainly have attracted far more attention but

for the fact that they are very difficult to prepare in the form of large crystals. Graphite differs from all the other semi-metals in having a very low atomic weight (thus reversing the tendency for the energy gap to rise as the atomic weight falls); in some respects graphite is an almost ideal semi-metal since it has electron and hole mobilities which are large and nearly equal. Grey tin, also, has comparable values for the mobility of the two types of carrier.

Turning to the compounds, the IV-VI semiconductors such as PbTe and PbS have been widely studied for many years. At least one of the IV-VI compounds, GeTe, is probably a true semi-metal and is especially interesting in that it can become superconducting at very low temperatures.

The II–VI compounds HgTe and HgSe are either semiconductors with extremely small energy gaps or, less probably, semi-metals with slightly overlapping bands. They, like the III–V compound InSb, have a very large ratio of electron to hole mobility and so do not display strong bipolar effects. On the other hand, the V–VI compounds, such as Bi₂Te₃ have mobility ratios that are much closer to unity and, in fact, it was with Bi₂Te₃ that the phenomenon of bipolar heat conduction was first demonstrated.

Although it is simpler from the experimental viewpoint to work with elements and compounds, there is considerable interest at the present time in solid solutions. The formation of a solid solution between two or more metals inevitably leads to a considerable reduction in the relaxation time of the charge carriers but this need not be so for solid solutions that are semi-metallic or semiconducting. Since such solid solutions can have high carrier mobilities they are just as suitable as the pure elements for many applications and they allow much greater flexibility in the choice of energy gap or band overlap. In fact, were it not for the technological difficulty of producing homogeneous solid solutions there would be a much more widespread use of their potentialities.

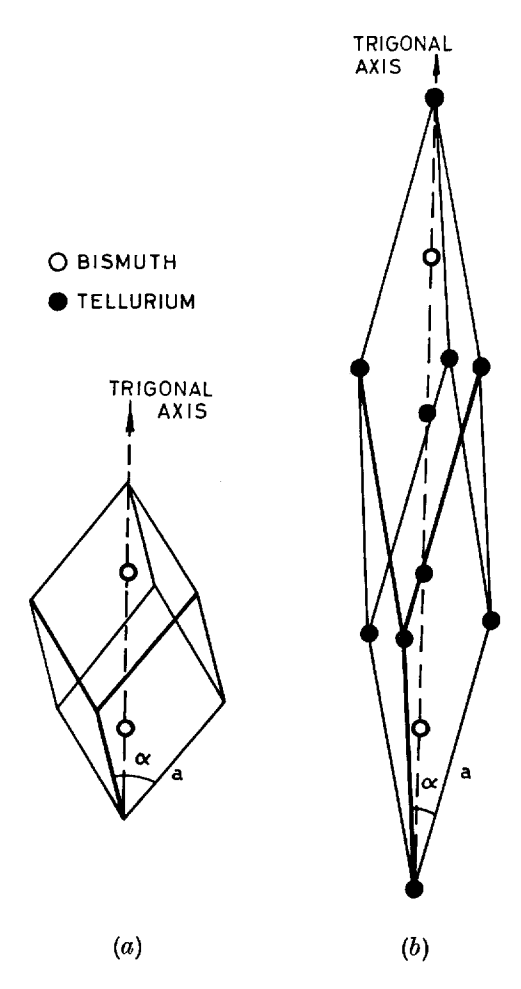
§ 2. Characteristics of Specific Materials 2.1. Crystal Structures

The materials that have been mentioned in the Introduction are more closely related to one another than might appear at first sight. This fact is brought out by a discussion of their crystal structures. The Group V elements, Bi₂Te₃ and GeTe all have the space group R3m.

Bismuth has a rhombohedral structure with a primitive trigonal cell as shown in fig. 2(a). The symmetry elements include three binary axes in a plane which is perpendicular to the single trigonal axis. There are three reflection planes which each contain the trigonal axis and a bisector of the angle between two of the binary axes. The lattice vectors a are each of length 4.75 Å and the trigonal angle α is equal to $57^{\circ}14'$, the two bismuth atoms being placed on the trigonal axis of the cell at a distance u, equal to 0.237a, from each of the vertices (Cucka and Barrett 1962). If this distance u were equal to 0.25a and if the trigonal angle were 60° , bismuth would possess a simple cubic structure. It will be realized, then, that the bismuth lattice is only slightly distorted from the cubic

configuration, though it must be emphasized that this does not imply that such transport properties as the thermal conductivity, are nearly isotropic.

Fig. 2



Trigonal unit cells for (a) bismuth (with a=4.75 Å and $\alpha=57^{\circ}$ 14') and (b) Bi₂Te₃ (with a=10.47 Å and $\alpha=24^{\circ}$ 10').

Arsenic (Wyckoff 1960) and antimony (Barrett et al. 1963) have the same structure as bismuth (which is, in fact, usually known as the arsenic structure) but the deviations from simple cubic are greater for these elements and the lattice dimensions are smaller. Bismuth and antimony form solid solutions in all proportions and there is also a complete range of solid solubility in the antimony–arsenic system. On the other hand bismuth and arsenic are only slightly soluble in one another (Wyckoff 1960).

Bi₂Te₃ also possesses a rhombohedral structure (Lange 1939). The trigonal cell contains two bismuth atoms and three tellurium atoms

arranged along the axis as shown in fig. 2(b). The positions of the atoms in the Bi₂Te₃ structure can be obtained from those in the bismuth structure simply by modifying the interatomic spacings in an appropriate fashion and, of course, substituting three-fifths of the bismuth atoms by tellurium atoms. Bi₂Te₃ has a melting-point maximum in the phase diagram close to the stoichiometric composition, but there is, nevertheless, a wide range of solid solubility in the Bi-Te system between bismuth and Bi₂Te₃ (Brown and Lewis 1962). Single-phase solid solutions have been found with all tellurium concentrations between 30 and 60 at. %. These intermediate alloys are rather difficult to prepare and have been little studied. Most of them are likely to be semi-metallic with far from equal concentrations of electrons and holes. Sb₂Te₃ has the same structure as Bi₂Te₃, and a range of solid solubility has been found by Brown and Lewis in the Sb-Te system which is even wider than that in the Bi-Te system. Bi₂Se₃ also has the structure of Bi₂Te₃.

A noteworthy feature of Bi₂Te₃ is that the crystals are composed of layers of atoms following the sequence -Te-Te-Bi-Te-Bi-Te-Te-, the spacing between the adjacent tellurium layers being abnormally large (note that the trigonal axis of the unit cell in fig. 2(b) extends over 15 layers). It appears that the binding electrons are used up in mixed covalent-ionic bonds between the bismuth and tellurium layers leaving only very weak van der Waals bonds between the neighbouring tellurium layers (Drabble and Goodman 1958). Thus Bi₂Te₃ can be cleaved even more readily than bismuth along planes perpendicular to the trigonal axis.

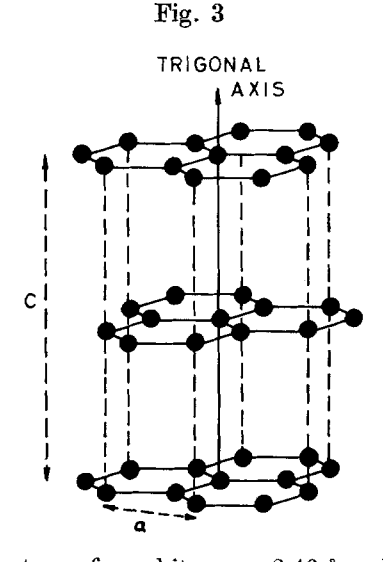
Table 1. Trigonal cell parameters of some semi-metals and related semiconductors

Element or compound	a Å	α
Bi	4.75	57° 14′
\mathbf{Sb}	4.51	57° 7′
As	4.13	54° 10′
GeTe	4.23	58° 15′
\mathbf{SnTe}	4.44	60°
${ m PbTe}$	4.55	60°
\mathbf{PbSe}	4.33	60°
${ m PbS}$	4.20	60°
$\mathrm{Bi}_{2}\mathrm{Te}_{3}$	10.47	24°10′
2 0		

PbTe, PbSe, PbS and SnTe all possess the rock-salt structure which may be regarded as a simple cubic structure with alternate sites occupied by atoms of a different type. Thus, a distortion of the rock-salt structure towards rhombohedral symmetry produces a structure analogous to that of bismuth having two types of atom. This distorted rock-salt structure is observed for the compound GeTe. It is interesting to note that, despite its rhombohedral structure, GeTe forms a complete range of solid solution

with SnTe, there being a gradual transition away from the cubic structure as the GeTe content is increased (Bierly et al. 1963). Similar solid solutions can be formed between GeTe and AgSbTe₂ which is a cubic ternary compound analogous to the rock-salt structured IV-VI compounds (Rosi et al. 1961); the structure remains cubic as GeTe is added to AgSbTe₂ until the former reaches a concentration of about 80 mol. %.

The trigonal cell parameters of most of the elements and compounds mentioned above are given in table 1. The fact that Bi₂Te₃ has a very different trigonal angle from the other materials is due primarily to the fact that the unit cell contains five instead of two atoms, though the rather long weak bonds between the tellurium layers in Bi₂Te₃ do imply that it is not quite so close to a cubic material as, say, bismuth or antimony. The implications of the similarities in crystal structures on the energy band structures have been discussed by Cohen et al. (1964).



Crystal structure of graphite. a = 2.46 Å and c = 6.74 Å.

Graphite is another material with a layer structure, and single crystals of it can be cleaved very easily along the basal planes. Its crystal structure is shown in fig. 3. Graphite is often regarded as a two-dimensional crystal since the inter-layer spacing of 3·37 Å is so much larger than the distance between nearest-neighbour atoms in each layer plane of 1·42 Å. Although the graphite structure is hexagonal rather than rhombohedral, its symmetry elements are not too dissimilar from those of bismuth or Bi₂Te₃. In particular, crystals of graphite are uniaxial with three-fold rotational symmetry about the axis which lies perpendicular to the planes of easy cleavage.

The other substances of interest to us all possess cubic structures derived from that of diamond. Grey tin, of course, actually has the diamond

structure, while HgTe and HgSe, like the III-V compounds, have the zinc-blende structure in which the alternate atoms are of a different type. There are a very large number of more complex compounds containing three or more elements that can be derived from the Group IV elements and III-V compounds by the rules of cross-substitution (Goodman 1958). Thus, by analogy with grey tin and InSb, one might expect CdSnSb₂ to be a narrow-gap semiconductor or perhaps a semi-metal, though in practice it does not seem possible to form this particular compound. Most of the work on the ternary and quaternary compounds and their solid solutions has been confined to the wider gap semiconductors but there are doubtless a large number of smaller gap materials that could be studied.

Except in purely qualitative work, it is usually essential to obtain single crystals of the rhombohedral and hexagonal materials mentioned above, and, even for the cubic materials, single crystals are highly desirable. It is beyond the scope of this article to describe the preparation of single crystals in detail but a few remarks may be helpful. Most of the materials that have been mentioned can be grown from the melt and an excellent review of the various techniques is that of Hurle (1963). Bismuth crystals are commonly grown by the Bridgman method using a soft mould of, for example, graphite powder to allow for the expansion or solidification. Strain-free single crystals of controlled orientation can be pulled from the melt (Porbansky 1959) the main difficulty arising from the reactivity of bismuth and its tendency to form an oxide scum on the liquid surface. The oxide can be removed by treatment in hydrogen at an elevated temperature; the crystal pulling is best carried out in vacuum. Directional freezing and zone-melting in horizontal boats have been carried out with varying Thus, Goss and Weintroub (1952) found that the movement of the interface at a slow speed leads to a lineage structure whereas, at a faster speed, the crystal breaks up into blocks differing to a greater or lesser extent in their orientation. On the other hand, Brown and Heumann (1946) have succeeded in producing single crystals of the Bi-Sb alloys by They were obliged to move the interface at less than zone melting. 1 mm/hr in order to avoid constitutional supercooling; the Bi-Sb alloys are characterized by a low diffusion coefficient, a segregation coefficient that is much greater than unity, and a low melting temperature, which makes it difficult to achieve a steep temperature gradient near the interface. Lacklison (private communication) has been able to pull a Bi-Sb alloy, containing 5 at. % of antimony, from the melt using a divided graphite crucible to maintain a constant composition of the solid in spite of the large segregation coefficient (5 to 10). The divided (or floating) crucible method has been described by Airapetyants and Shmelev (1960).

The techniques adopted for the other elements, compounds and solid solutions are often similar to those mentioned above, though in certain cases the presence of a volatile constituent (such as selenium or tellurium) introduces difficulties. It is not easy to obtain large single crystals of arsenic since it sublimes at atmospheric pressure. However, it can be

melted at some 820°C if a pressure of about 36 atmospheres is maintained. Saunders and Lawson (1965) have succeeded in growing large crystals from the melt under the vapour pressure of the arsenic itself.

Some of the compounds have melting-point maxima that are not precisely at the stoichiometric composition; thus, growth of crystals from the stoichiometric melt produces a non-stoichiometric solid which displays extrinsic rather than intrinsic conduction.

Graphite, of course, present special problems. Some work has been done using natural crystals of graphite but these are always very small. Larger samples with near-single crystal properties can be prepared by pyrolytic deposition followed by reheating at up to 3600°c (Klein et al. 1962). It is also extremely difficult to obtain single crystals of grey tin, on account of its phase change to the metallic form at 13·2°c. Van Leut (1962) has, however, managed to produce crystals, that are relatively pure and perfect, from mercury-rich Hg–Sn alloys.

2.2. Electronic Parameters

The transport properties of a conductor depend, in general, on the mobilities of the different types of charge carrier and on their effective mass tensors, in so far as it is legitimate to use the concept of an effective mass. They depend on the positions in **k** space of the extrema of the conduction and valence bands, since these positions determine the multiplicity of the constant-energy surfaces according to the crystal symmetry. In addition, unless the material is perfectly pure (and stoichiometric if it is a compound), it is necessary to know the excess or deficiency of electrons as compared with holes; alternatively the position of the Fermi level with respect to the band extrema could be specified. The thermal properties also involve the lattice contribution to the heat conductivity.

The qualification, in the preceding paragraph, in connection with the use of an effective mass, is particularly significant for a narrow-gap material. Even for a wide-gap semiconductor such as germanium or silicon, there are noticeable departures from parabolicity in the bands when the carrier concentration exceeds about $10^{18}/\mathrm{cm}^3$ (Cardona et al. 1960). Non-parabolic effects become important for narrow-gap semiconductors at appreciably lower carrier concentrations because of the strong interaction between the valence and conduction bands when their edges are close to one another. It seems certain that one should use non-parabolic band models for most, if not all, of the materials discussed here but it is quite common to interpret the experimental results in terms of a pseudo-parabolic model, the effective mass then being a function of the Fermi energy.

There are, of course, band extrema at energies which differ from those at the conduction band minimum and the valence band minimum. When the carrier concentration is small these other extrema can be ignored, but for the high carrier concentrations encountered in semi-metals, they may well account for appreciable numbers of carriers. This will be so particularly if the additional extrema have energies that are not widely

different from those of the principal extrema and if they have large effective mass values associated with them.

A considerable effort has been devoted to the determination of the energy band structure of bismuth by a variety of experimental techniques, these results the surfaces of constant energy will be referred to as electron and hole ellipsoids although it must be accepted that the electron surfaces are not strictly ellipsoidal and the conduction band is non-parabolic (Lax et al. 1960, Cohen 1961). In general, the experiments can be explained in terms of three or six light-electron ellipsoids and one or two light-hole ellipsoids of revolution about the trigonal axis, while some workers have invoked additional carriers—the so-called heavy holes (Lerner 1962, 1963). Each electron ellipsoid is tilted in \mathbf{k} space with respect to the crystallographic axes by some 5° about a binary axis, though in the useful Abeles and Meiboom (1956) model this tilt is ignored. It is easy to be confused by the manifold data that are available, but Jain and Koenig (1962) have presented clear arguments that seem to establish the true picture. They pointed out that such phenomena as the de Haas-van Alphen effect, and others in which oscillatory behaviour is observed as the magnetic field is varied, vield the carrier concentration per ellipsoid whereas Hall effect measurements, for example, give the total carrier concentration. Jain and Koenig found that these two types of measurement are consistent with one another only if it is assumed that there are three electron ellipsoids and it is presumed that these are, in fact, six half-ellipsoids centred at the Lpoints at the surface of the Brillouin zone (see fig. 4) as suggested by band structure calculations. Within each valley the effective mass is low in the binary axis direction and along the axis which is nearly parallel to the trigonal axis, while it is high along the axis which is nearly parallel to a bisectrix direction. For pure bismuth at 0° k there are about 1.4×10^{17} electrons per ellipsoid/cm³ and about 4×10^{17} electrons/cm³ altogether. Although fewer data are available for holes, it seems established that there can be only one light-hole spheroid, or rather two half-spheroids centred at the point T on the Brillouin zone surface. The measurements show that the hole effective mass is much higher along the direction of the trigonal axis than in the binary-bisectrix plane. Jain and Koenig showed that there can be only a very small number of heavy holes (if any) at low temperatures though it is by no means certain that the light electrons and holes are the only carriers at room temperature (Gallo et al. 1963).

Since we are concerned here with the transport properties of bismuth it is particularly relevant to consider the energy band data that result from transport measurements. The comprehensive measurements of the magneto-thermoelectric and galvanomagnetic effects by Smith, Wolfe and Haszko (1964) were analysed in terms of a non-parabolic electron band of the form (Cohen 1961):

$$E\left(1 + \frac{E}{E_{\rm G}}\right) = \frac{\hbar^2 \mathbf{k} \cdot \mathbf{m}^{*-1}, \mathbf{k}}{2}, \dots$$
 (2)

where $E_{\rm G}$ is the direct energy gap. The valence band is supposed to be parabolic so that for the holes

$$-E_g - E = \frac{\hbar^2 \mathbf{k} \cdot \mathbf{m}^{*-1}, \mathbf{k}}{2}, \quad (3)$$

 $-E_g$ being the band overlap, and the energy being taken as zero at the conduction band edge. The results of Smith and his colleagues at 80° K are shown in table 2, which also gives the data of Abeles and Meiboom combined with those of Gallo *et al.* (1963). In view of the different assumptions, the poor agreement between the two sets of parameters is hardly surprising.

Table 2. Band parameters of bismuth derived from transport measurements at 80°K. Set I refers to Smith, Wolfe and Haszko (1964) while set II refers to Abeles and Meiboom (1956) and Gallo *et al.* (1963)

	Electron masses			Hole masses		Direct gap	Band overlap	
	m_{11}/m	m_{22}/m	m_{33}/m	m_{23}/m	M_1/m	M_3/m	E_{G}	$-E_g$
I† II‡	0·002 0·013	0·15 0·53	0·005 0·022	-0.015	0·075 0·077	0·5 0·29	15 mev	44 mev 32 mev

[†] Non-parabolic, tilted band.

The conclusions of both Smith *et al.* and Gallo *et al.* were based on the assumption of isotropic relaxation times for the charge carriers, the expressions for the relaxation times of electrons and holes being:

and

respectively, A and λ being constants. Smith found that his results could be fitted best by assuming $\lambda_e = \lambda_h = -0.2$, this being appropriate for acoustic-mode lattice scattering, though other workers have used the value -0.5 for the exponent in the relaxation time expressions. The term 'mobility' does not have the same significance for a partially degenerate conductor as it does for a lightly doped semiconductor, since it becomes a function of the Fermi energy if classical statistics cannot be employed. However, some idea of the magnetic fields that are necessary to produce high-field effects can be obtained from the mobilities quoted for a sample of some arbitrary doping level. Table 3 gives values for the mobilities of electrons and holes in bismuth, in the direction of the trigonal axis and perpendicular to this direction, at three specific temperatures, according to Abelés and Meiboom (1956) and Zitter (1962).

[‡] Parabolic, non-tilted band.

Turning now to antimony, there are a number of qualitative differences from bismuth that are readily apparent. The electron mobilities are appreciably smaller for antimony while the carrier concentrations are much Thus, at room temperature the concentration of electrons or holes in antimony is about $4 \times 10^{19} / \text{cm}^3$ (Epstein and Juretschke 1963) whereas in bismuth it is only about $2 \times 10^{18}/\text{cm}^3$ (Abeles and Meiboom 1956).

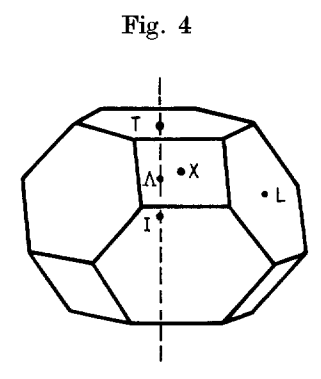
Table 3. Mobilities of electrons and holes in intrinsic bismuth. values at 4.2°K are due to Zitter (1962) while those at 80°K and 300°K are due to Abeles and Meiboom (1956). All values are given in $cm^2/v sec$

Carrier	Direction	4·2°ĸ	80°ĸ	300°ĸ
Electrons Electrons Holes Holes	trigonal trigonal trigonal trigonal	30×10^{6} 22×10^{6} 10^{6} 12×10^{6}	$\begin{array}{c} 33 \cdot 3 \times 10^4 \\ 28 \cdot 6 \times 10^4 \\ 3 \cdot 33 \times 10^4 \\ 12 \cdot 4 \times 10^4 \end{array}$	$ \begin{array}{c c} 19 \times 10^{3} \\ 16 \cdot 3 \times 10^{3} \\ 2 \cdot 1 \times 10^{3} \\ 7 \cdot 7 \times 10^{3} \end{array} $

The possible band models for antimony have been reviewed by Hall and Koenig (1964). All experiments indicate that the electron ellipsoids (which are deduced to be three in number and probably situated at the X points on the Brillouin zone face) are tilted by an appreciable angle about the binary axes in a sense opposite to that for bismuth. Cyclotron resonance measurements (Datars and Dexter 1961) give effective mass values $m_1 = 0.06m$, $m_2 = 1.8m$ and $m_3 = 0.05m$ within the principal axis system of each ellipsoid, the angle of tilt being 36°. The situation for the valence band is far less clear. Hall and Koenig suggest that some 70% of the holes have prolate ellipsoidal surfaces of constant energy, centred on the trigonal axis probably at the T points on the Brillouin zone face, while the remaining holes are accounted for by oblate ellipsoids, also centred on the trigonal axis at two A points (see fig. 4). On the other hand, the galvanomagnetic measurements of Freedman and Juretschke (1961) and of Epstein and Juretschke (1963) are more consistent with three or six tilted hole ellipsoids. Recent cyclotron resonance measurements by Datars and Vanderkooy (1964) also show that there are three (warped) hole ellipsoids, though their tilt angle of 4° is rather less than the 20-30° obtained from the galvanomagnetic coefficients. Whatever the true valence band structure, certain qualitative features of Epstein and Juretschke's conclusions must hold good. Thus, they show that the band overlap is about 190 mev and the electron and hole mobilities are both of the order of 103 cm²/v sec at room temperature, in any particular direction.

There has been relatively little work on the third of the semi-metallic Group V elements, arsenic. Band structure calculations (Falicov and Golin 1965) indicate close similarities with bismuth, the holes being located at the T point and the electrons near the L points in the Brillouin zone.

As might be expected, the Group IV elements, such as tin, act as acceptor impurities in the Group V semi-metals while the Group VI elements, such as tellurium act as donors. The addition of one of the Group V elements to another does not, of course, disturb the equality of the electron and hole concentrations but it does lead to interesting changes in the band structure. Jain (1959) first showed, from measurements of the Hall effect and electrical conductivity as a function of temperature, that the addition of between 5 at. % and 40 at. % of antimony to bismuth changes it from a semi-metal to a semiconductor. Figure 5 shows Jain's plot of E_g , the minimum energy gap, against composition. There are some indications that the energy gap may be even greater than 14 mev for composition containing between 10 and 20 at. % of antimony; Brown and Silverman (1964) deduced a value of 24 mev from the temperature variation of the resistivity of the Bi₈₅Sb₁₅ alloy.



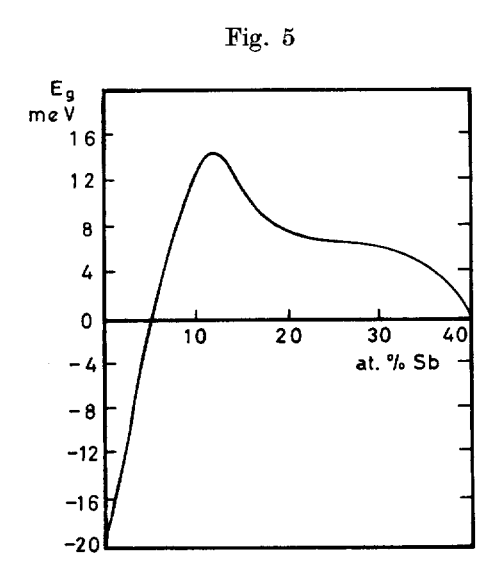
Schematic drawing of the first Brillouin zone for the Group V semi-metals and the V_2VI_3 semiconductors with the R3m space group.

The effect of adding bismuth to antimony is to raise the value of the direct gap at the X points through an increase in the lattice potential and to decrease the gap at the L points through an increase in the spin-orbit coupling. Presumably the minimum energy gap E_g reaches its highest value when the maximum energy of the valence band, or the minimum energy of the conduction band, is just shifting from the position it occupies for pure antimony to some other part of the Brillouin zone. If Hall and Koenig's interpretation of the band structures of bismuth and antimony is correct, then E_g has its largest value when the electrons at the X and L points have the same energy.

It must be emphasized that there is an important difference between the effects of forming alloys or solid solutions between semiconductors or semi-metals, on the one hand, and between metals, on the other. The scattering of the charge carriers is always much stronger for a disordered metal alloy than it is for a metallic element or compound. However, the carrier mobilities in disordered solid solutions between semiconductors are generally of the same order as those in the pure elements or compounds. This is because the wavelengths of the electrons in semiconductors and semi-metals are very much greater than the interatomic spacing, so that disturbances in the short range order do not lead to appreciable scattering. Thus, the carrier relaxation times at $1\cdot 3^{\circ} \kappa$ are long enough in a $\mathrm{Bi}_{95}\mathrm{Sb}_5$ alloy for Smith (1962) to have been able to observe cyclotron resonance. Smith found that the electron effective masses for this alloy were smaller than those in bismuth by a factor of two whereas the hole effective masses were the same as for bismuth. If it is supposed that the only effect of

alloying is to move the bands relative to one another, this provides good

evidence for the non-parabolicity of the conduction band.



Energy gap plotted against antimony concentration in Bi-Sb alloys according to Jain (1959).

A study of the alloys between arsenic and antimony by Saunders *et al.* (1965) has shown that these are semi-metallic at all compositions, the band overlap rising from 190 mev for antimony to 370 mev for arsenic.

The general features of the band structure of Bi₂Te₃ were first obtained by Drabble (1958) and by Drabble et al. (1958) from the analysis of the galvanomagnetic effects at liquid nitrogen temperature. The simplest model that could account for the observed properties was found to involve three or six valleys for both the conduction and valence bands. As for electrons in bismuth or antimony, the surfaces of constant energy are ellipsoids that are rotated about the binary axes. The electron ellipsoids are almost spheroidal about an axis almost parallel to the trigonal axis and are highly compressed in this direction. The hole ellipsoids, too, are almost spheroidal, being highly compressed in the directions of the binary axes. Studies by Sehr and Testardi (1963) of the reflection minima associated with the free-carrier plasma edges have indicated that

there are six rather than three valleys for both bands, this being consistent for the valence band with the de Haas-van Alphen data obtained by Testardi et al. (1962).

Drabble's analysis was based on the assumption of a quadratic relation between energy and wave-vector but, in view of the high carrier concentrations that are always encountered in Bi₂Te₃, this is questionable. measurements of the galvanomagnetic properties of strongly doped n-type material (Delves et al. 1961) can only be interpreted in terms of a six-ellipsoid model if a different effective mass tensor from that used by Drabble is employed; this is another way of saying that the conduction band is non-parabolic. Drabble also assumed the relaxation time to be isotropic; strictly speaking, the galvanomagnetic measurements determine the combined anisotropy of effective mass and relaxation time within a A further complicating feature may be valley (Efimova et al. 1962). the presence of carriers in a second conduction band having a minimum that is not much higher than that of the lowest conduction band minimum. The second conduction band has been invoked by Ure (1962) to explain his measurements on uncompensated n-type Bi_2Te_3 .

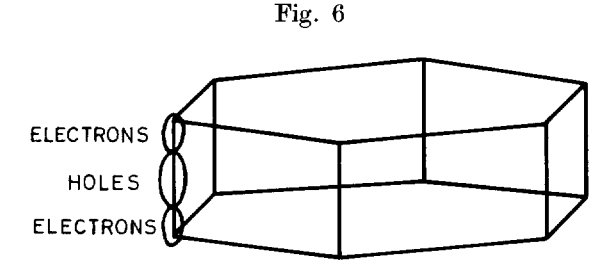
The minimum energy gap E_g for $\mathrm{Bi}_2\mathrm{Te}_3$ at $0^\circ\mathrm{K}$ is 150 mev (Austin 1958). The electron and hole mobilities perpendicular to the trigonal axis are about $1200~\mathrm{cm}^2/\mathrm{v}$ sec and $500~\mathrm{cm}^2/\mathrm{v}$ sec at $300~\mathrm{K}$ (Goldsmid 1962) and the corresponding density of states effective masses are 0.6m and 1.1m. It is this combination of properties that ensures appreciable contributions to the electrical conductivity from both the electrons and holes in intrinsic material, $\mathrm{Bi}_2\mathrm{Te}_3$ thus exhibiting strong bipolar effects. Another significant feature of $\mathrm{Bi}_2\mathrm{Te}_3$ is the fact that its electron or hole mobility increases monotonically as the temperature is lowered, its value tending towards some limit that is characteristic of the degree of perfection of the particular sample. In all specimens that have been studied to date the carrier concentration remains finite at $0~\mathrm{K}$; thus, $\mathrm{Bi}_2\mathrm{Te}_3$ invariably displays a residual resistance effect similar to that encountered for a metal.

Galvanomagnetic measurements on n-type Bi_2Se_3 have yielded a six-valley conduction band model as for Bi₂Te₃ (Hashimoto 1961). Austin and Sheard (1957) have determined the energy gap of Bi₂Te₃-Bi₂Se₃ alloys from optical absorption measurements. They found that the energy gap of Bi₂Te₃ rises on the addition of up to about 30 molar % Bi₂Te₃, but further additions lead to a reduction in the gap. Such a discontinuity in the slope of a plot of energy gap against composition usually indicates a change in the location in the Brillouin zone of either the valence or conduction There may, however, be another explanation of Austin band extrema. and Sheard's observations. It has been suggested that, when some of the tellurium atoms in Bi₂Te₃ are replaced by selenium atoms, the latter go preferentially on to sites in the tellurium layers that lie between the bismuth layers (see § 2.1) (Drabble and Goodman 1958). Of course, this process can only continue until all these sites are filled, that is at the composition Bi₂Te₂Se; one might, therefore, expect a discontinuity at this composition.

If Drabble and Goodman's suggestion is correct, Bi₂Te₂Se should behave as an ordered solid solution. Misra and Bever (1964) have produced evidence that ordering occurs if samples of Bi₂Te₂Se are annealed for a sufficiently long period, but transport measurements have not been carried out on material that is known to be ordered.

Sb₂Te₃, like Bi₂Se₃ forms solid solutions with Bi₂Te₃ in all proportions. The properties of holes in Sb₂Te₃ are similar to those in Bi₂Te₃ but the electron characteristics are not known, since the compound is always far from stoichiometric, with a high acceptor concentration due to the excess antimony. For the same reason the energy gap of Sb₂Te₃ is unknown but it is certainly very small and possibly zero.

Since GeTe has a crystal structure that is so little distorted from that of the cubic IV–VI compounds, it might be expected that its electronic properties would be similar to those of PbTe, PbSe and PbS. The three latter compounds all have energy gaps of about 0·3 ev and mobilities for electrons and holes of the order of 1000 cm²/sec. However, in practice the properties of GeTe are quite different. It is always non-stoichiometric and strongly p-type, so attention has been confined to the hole characteristics. The hole mobility is no more than 50 cm²/v sec, the effective mass being correspondingly large, of the order of twice the free electron mass (Moriguchi and Koga 1957). That GeTe is a semi-metal rather than a semiconductor has been inferred from the values of the Seebeck coefficient which are small even at elevated temperatures. The fact that the carrier concentration in GeTe is always so high makes the question of whether or not it is a semi-metal of hardly more than academic interest.



The Brillouin zone and part of the Fermi surface shown schematically for graphite. There are similar parts of the Fermi surface at each of the six edges. The warping of the surfaces is not illustrated.

The energy band structure of graphite is rather complex because of the close proximity, at the edge of the Brillouin zone, of the Fermi surfaces for electrons and holes. The Fermi surfaces are shown schematically as ellipsoids at zone edge of the Brillouin zone in fig. 6 but, in fact, both sets of surfaces are severely warped (McClure 1964). The effective masses of both types of carrier are of the order of 0.05m perpendicular to the trigonal axis and an order of magnitude higher in the direction of the trigonal axis. The band overlap is about 30 mev as deduced from the de Haas—van Alphen data (Soule 1958).

In spite of the complexity of the constant-energy surfaces, Klein (1964) has shown that the transport properties of well-annealed pyrolytic graphite can be interpreted using a simple two-band (STB) model. are assumed to be parabolic with cylindrical energy surfaces and a small overlap in energy between the band edges for the pure material. Within the terms of this model the values of the overlap energy $-E_{a}$ and the effective masses must be regarded as phenomenological parameters chosen to agree with the transport coefficients and not necessarily related in any simple fashion to the parameters determined from de Haas-van Alphen oscillations or other effects. Klein's results, can, in fact, be fitted by the STB model if the band overlap is supposed to be 10 mev and the effective masses are equal to 0.0125m. The mobility of both types of carrier in the layer planes is about $10^4 \,\mathrm{cm^2/v}$ sec at room temperature rising to about $10^6 \,\mathrm{cm^2/v}$ sec for reasonably good samples at very low temperatures. The mobility ratio μ_e/μ_h is about 1·1 at room temperature but appears to vary somewhat with temperature.

It might have been expected that the properties of grey tin and InSb would be very similar to each other in view of the fact that indium and antimony lie next to tin in the periodic table. There are, however, marked differences between their electronic properties. InSb has an energy gap of 170 mev with an electron mobility of more than 70 000 cm²/v sec, though the hole mobility is only about 1000 cm²/v sec. On the other hand, the mobilities of electrons and holes in grey tin are very similar to one another; both are equal to about 100 cm²/v sec at room temperature (Busch and Wieland 1953). The energy gap of grey tin is 90 mev (Busch and Kern 1960). The effective mass of electrons in InSb is about 0.01mwhile in grey tin it is of the order of the free electron mass. clear, then, that the reason for the differences between InSb and grey tin is likely to be found in their having different conduction band structures. Since InSb has its conduction band minimum at k = 0, we can expect grey tin to possess a multi-valley conduction band. This has been confirmed by Paul (1961) whose high pressure experiments suggest that the minima lie at the edges of the Brillouin zone in the $\langle 111 \rangle$ directions.

The two mercury compounds HgSe and HgTe are characterized by very high electron mobilities and much smaller hole mobilities. Although some workers have given rather large values for the energy gap of HgSe, it seems much more likely that the gap is smaller for both compounds. Thus, Rodot et al. (1961) state that the energy gap of HgTe is 25 mev while that of HgSe is less than 80 mev. It appears that for both materials the energy band minima occur at $\mathbf{k} = 0$, the effective masses being about 0.03m to 0.05m, but varying with carrier concentration since the bands are non-parabolic. At 300° K, the electron mobility in HgTe normally exceeds $20\,000\,\mathrm{cm^2/v}$ sec (the mobility ratio b being equal to about 70) while for HgSe the electron mobility is about $10\,000\,\mathrm{cm^2/v}$ sec.

One narrow-gap semiconductor that has not so far been mentioned is Cd_3As_2 which has a tetragonal structure and E_q equal to 130 mev (Turner

et al. 1961). What makes this material interesting is its high electron mobility of $15\,000\,\mathrm{cm^2/v}\,\mathrm{sec}$ at room temperature as determined for a sample containing 2×10^{18} carriers/cm³. This combination of high mobility and high extrinsic carrier concentration may well make more intensive studies of $\mathrm{Cd_3As_2}$ worth while.

§ 3. Transport Phenomena in the Absence of a Magnetic Field

3.1. Thermoelectric Effects and Heat Conduction

Before dealing with the more general situation of the transport phenomena in combined electric and magnetic fields and a thermal gradient, we shall consider the interesting effects that occur in the absence of a magnetic field.

The transport properties in zero magnetic field for a single-band or extrinsic conductor are determined by the substitution of the appropriate band parameters in certain well-known equations (Wilson 1953). Briefly, for electrons, the electric current density is:

,
$$j = -\int_0^\infty eufg \, dE$$
, (6)

where e is the electronic charge, u is the electron velocity, f is the Fermi distribution function and g is the density of states at the energy E. The rate of flow of heat per unit cross-section area due to the electrons is:

$$w = \int_{0}^{\infty} u(E - \zeta) fg \, dE, \qquad (7)$$

where ζ is the energy at the Fermi level, otherwise known as the electrochemical potential. There is an additional contribution to the heat flow from the lattice vibrations.

Incidentally, it is supposed that the flows in the systems of electrons and lattice vibrations are independent of one another, apart from the scattering of electrons by phonons and vice versa. In other words, we do not include the phonon-drag effects (Gurevich 1945, Herring 1958). It seems that the neglect of the phonon-drag effects is generally valid for the types of material under discussion here, for a number of reasons. The materials tend to have large electron mobilities and small lattice Thus, the relaxation time for scattering of thermal conductivities. electrons by phonons is long and the relaxation time for scattering of the phonons tends to be short (though it must be remembered that it is different groups of phonons that are primarily responsible for the conduction of heat and for phonon drag respectively). Moreover, even if conditions were otherwise suitable for phonon drag to occur, the effect would be diminished by the presence of large carrier concentrations (the so-called saturation effect). When the carrier concentration is high, much of the momentum that is passed on from the electrons to the phonons is returned subsequently from the phonons to the electrons.

Since we are not at the moment interested in the non-parabolic nature of the density-of-states function, we can adopt a constant effective mass m^* . We treat this as a scalar quantity here since we are not concerned for the present with the more general tensor properties. Then the density-of-states function is:

$$g = \frac{4\pi (2m^*)^{3/2} E^{1/2}}{h^3} \qquad . \qquad (8)$$

and

$$u^2 = \frac{2E}{3m^*} \cdot \qquad (9)$$

Substitution in eqns. (6) and (7) yields:

$$\sigma = \frac{e^2}{T} K_0, \qquad (10)$$

$$\alpha = \frac{1}{eT} \left(\zeta - E_c - \frac{K_1}{K_0} \right) \quad . \quad . \quad . \quad . \quad (11)$$

and

$$\kappa_{\rm E} = \frac{1}{T^2} \left(K_2 - \frac{K_1^2}{K_0} \right), \quad (12)$$

where σ is the electrical conductivity, α is the Seebeck coefficient and $\kappa_{\rm E}$ is the electronic thermal conductivity. E_c is the energy at the edge of the conduction band and the integrals K_s are defined by:

where

$$K_s = \frac{8\pi}{3} \left(\frac{2}{h^2}\right)^{3/2} m^{*1/2} T A(s+\lambda+\frac{3}{2}) (kT)^{s+\lambda+\frac{3}{2}} F_{s+\lambda+\frac{1}{2}}, \tag{13}$$

 f_0 being the equilibrium Fermi distribution function, and where it has been assumed that the relaxation time may be expressed as in eqn. (4). The ratio $\kappa_{\rm r}/\sigma T$, known as the Lorenz number, is thus given as:

$$L = \frac{1}{e^2 T^2} \left(\frac{K_2}{K_0} - \frac{K_1^2}{K_0^2} \right). \tag{15}$$

For conduction by holes eqn. (15) is still applicable but eqn. (11) must be modified to:

$$\alpha = \frac{1}{eT} \left(\zeta - E_v + \frac{K_1}{K_0} \right), \quad . \quad . \quad . \quad . \quad (11')$$

where E_v is the energy at the edge of the valence band. This implies that the Seebeck coefficient is positive for hole conduction whereas it is negative for electronic conduction. The magnitude of the Seebeck coefficient is directly proportional to a suitable average of the energy of the charge carriers measured with respect to the Fermi level. Thus, for a classical electronic semiconductor, the Seebeck coefficient is $\{\zeta - E_c - (\frac{5}{2} + \lambda)kT\}/eT$ where $\zeta - E_c$ can be regarded as the potential energy and $(\frac{5}{2} + \lambda)kT$ as the appropriate average of the kinetic energy.

The Lorenz number L is equal to $(\pi^2/3)(k/e)^2$ for a completely degenerate conductor and to $(\frac{5}{2} + \lambda)(k/e)^2$ for a classical semiconductor in which the assumptions outlined above are valid. Thus, for all extrinsic conductors, whether degenerate or non-degenerate, the Lorenz number is expected to have a comparatively small range of values, say from $2(k/e)^2$ to $4(k/e)^2$.

Where there is more than one band of carriers, the contributions of each band to the flows of charge and heat must be added together. It may be that there are two or more conduction (or valence) bands with energy maxima (or minima) at different levels. The following treatment (Drabble and Goldsmid 1961) is applicable in this case, but it is more interesting to apply it to the case of one electron band and one hole band. This is the normal situation for a mixed semiconductor or semi-metal. The electron band will be denoted by the subscript e and the hole band by the subscript h.

The equations for the partial flows of current and heat due to the two types of carrier are:

$$\mathbf{i}_{e,h} = \frac{\sigma_{e,h} \operatorname{grad} \zeta}{e} - \sigma_{e,h} \alpha_{e,h} \operatorname{grad} T$$
 . . . (16)

and

$$\mathbf{w}_{e, h} = \left(\pi_{e, h} - \frac{\zeta}{e}\right) \mathbf{i}_{e, h} - \kappa_{e, h} \operatorname{grad} T, \quad . \quad . \quad . \quad (17)$$

 π being the Peltier coefficient.

The electrical conductivity of the mixed conductor is given by the ratio of the electric current to the gradient of the electrochemical potential when the temperature gradient is zero. Quite simply:

The Seebeck coefficient is determined by setting the total current equal to zero, i.e. $\mathbf{i}_e = -\mathbf{i}_h$, whence

$$\alpha = \frac{\alpha_h \sigma_h + \alpha_e \sigma_e}{\sigma}. \qquad (19)$$

Since α_e and α_h are of opposite sign, the Seebeck coefficient of a mixed conductor is generally small compared with that of an extrinsic conductor.

The electronic thermal conductivity is found by summing \mathbf{w}_e and \mathbf{w}_h for the condition that the total current is zero. Thence, it is found that:

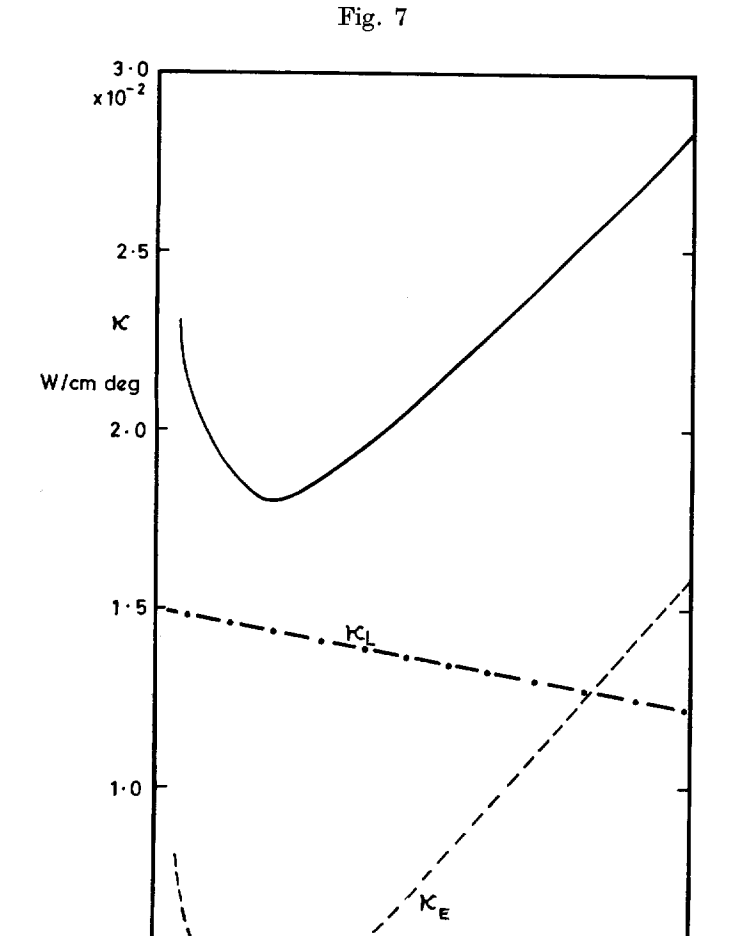
$$\kappa_{\rm E} = \kappa_e + \kappa_h + \frac{\sigma_e \sigma_h}{\sigma} (\alpha_h - \alpha_e)^2 T \qquad . \qquad . \qquad . \qquad (20)$$

and the Lorenz number is

$$L = \frac{L_e \sigma_e + L_h \sigma_h}{\sigma} + \frac{\sigma_e \sigma_h}{\sigma^2} (\alpha_h - \alpha_e)^2. \qquad (21)$$

It is, at first sight, rather surprising that the electronic thermal conductivity is not simply the sum of the separate contributions from the two bands. The additional term arises from the fact that electron and holes can move together in the same direction, transporting energy but not carrying any net charge.

The Lorenz number can be very large for an intrinsic wide-gap semi-conductor. Thus, if the mobilities and concentrations of the two types of carrier are more-or-less equal, the bipolar term in eqn. (21) is equal to about $(\alpha_h - \alpha_e)^2/4$, which is $(E_g/kT + 5 + \lambda_e + \lambda_h)^2(k/e)^2/4$ if classical



Thermal conductivity plotted against electrical conductivity for ${\rm Bi_2Te_3}$ at $300^\circ\kappa$. The lattice and electronic components are shown by the broken lines.

σ ohm-1 cm-1²

3 x 10 ³

0.5

statistics can be employed. Typically, with E_g of the order of 1 ev, the

bipolar Lorenz number at room temperature is no less than about $400(k/e)^2$. However, the electrical conductivity is so small for such a material that the electronic thermal conductivity is negligible compared with the lattice Bipolar heat conduction is much more easily observed for narrow-gap semiconductors in which the intrinsic electrical conductivity is relatively large.

Bipolar heat conduction was first suggested as an explanation of what was apparently a very large value for the thermal conductivity of InSb (Fröhlich and Kittel 1954) but subsequent work (Busch et al. 1959) showed that the bipolar effect is not normally appreciable for this compound. This is because the electron mobility of InSb is about 70 times as large as the hole mobility; thus, the ratio $\sigma_e \sigma_h / \sigma^2$ falls from the value of $\frac{1}{4}$, that it would have for an intrinsic material with equal carrier mobilities, to about $\frac{1}{20}$. It is, in fact, possible to obtain a high bipolar Lorenz number for InSb, or any similar compound with a high ratio of electron to hole mobility, if it is doped with acceptors so that the ratio of the concentration of holes to that of electrons is equal to the ratio of the electron mobility to the hole mobility. When this condition holds the ratio $\sigma_e \sigma_h / \sigma^2$ does attain the value of $\frac{1}{4}$. The required condition should obtain for any p-type sample at a specific temperature somewhat below that at which the conduction is effectively intrinsic.

The bipolar heat conduction effect can be demonstrated very easily with the compound Bi₂Te₃ (Goldsmid 1956). The lattice thermal conductivity is no more than about 0.015 w/cm deg at room temperature, while the electrical conductivity of intrinsic material is as high as 140 ohm⁻¹ cm⁻¹, the energy gap being only about 0.13 ev. The ratio of the mobilities of electrons and holes is little more than 2:1 which means that $\sigma_e \sigma_h / \sigma^2$ has not fallen much below $\frac{1}{4}$. Some experimental results for extrinsic and intrinsic Bi₂Te₃ are shown in fig. 7. In the extrinsic region, as the concentration of dopant increases, the thermal conductivity rises with electrical conductivity, the Lorenz number being given by eqn. (15), λ having the value of $-\frac{1}{2}$. However, in the intrinsic region the thermal conductivity again rises and it is found that the Lorenz number for the intrinsic compound is about $25(k/e)^2$. This is in good agreement with the value of $23.5(k/e)^2$ predicted by eqn. (21).

Gallo et al. (1962) have pointed out that bipolar heat conduction is not confined to semiconducting materials, but it may also be significant for semi-metals. This is quite clear from eqn. (21) since the difference $\alpha_h - \alpha_e$ between the partial Seebeck coefficients of holes and electrons does not vanish when the valence and conduction bands overlap. example, the bipolar contribution is more than 20% of the total electronic thermal conductivity, if the band overlap is less than 8kT, for $\lambda = -\frac{1}{2}$, or less than 20kT, for $\lambda = \frac{3}{2}$.

Gallo et al. (1963) took account of the bipolar effect for bismuth in the analysis of measurements of the electrical conductivity, Seebeck coefficient and thermal conductivity on single crystals. They determined these properties with the applied electrical or thermal gradients in both the direction of the trigonal axis and in the perpendicular direction. Since the thermoelectric properties depend primarily on the energies of the charge carriers, Gallo and his colleagues were able to calculate the band overlap and the position of the Fermi level from their results.

The significance of the bipolar contribution to the thermal conductivity to a semi-metal has also been discussed in relation to graphite by Klein and Holland (1963). At ordinary temperatures the lattice thermal conductivity along the layer planes of graphite is so large that the electronic contribution can be neglected, but at very low temperatures the fall in the specific heat is accompanied by a fall in the lattice conductivity. Thus at 2° K, nearly half the heat conduction is due to the charge carriers. However, at such low temperature, even with an energy band overlap of no more than about $10 \, \text{mev}$, this is so very much larger than kT that the bipolar contribution is negligible.

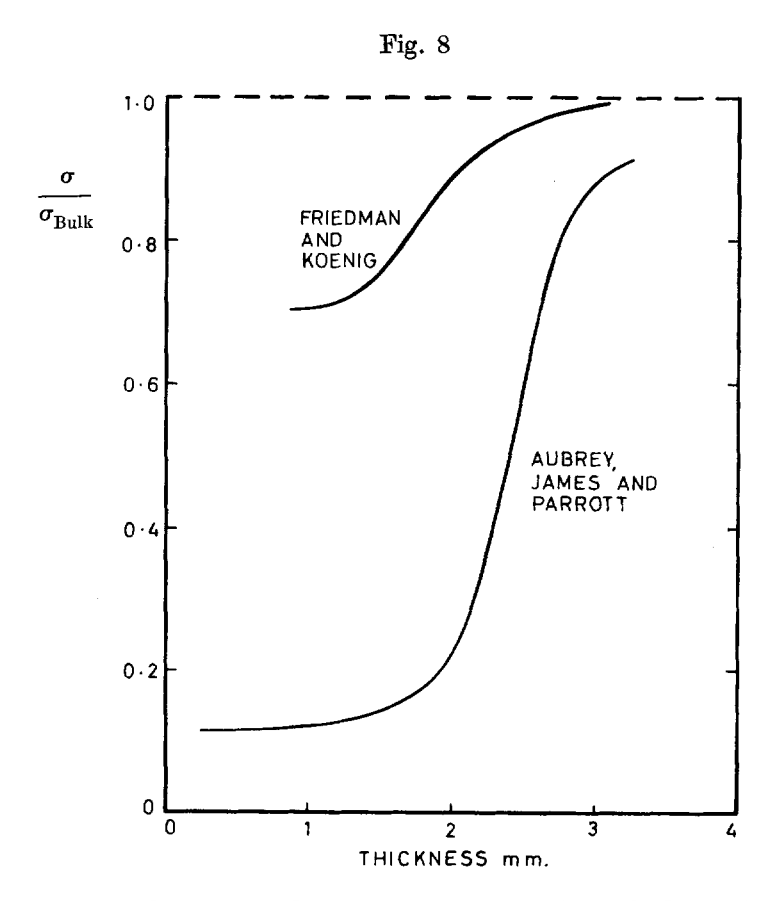
3.2. Size Effect on the Electrical Conductivity

If charge carriers are scattered diffusely at the surface of a conductor, one certainly expects the electrical conductivity to become size dependent when the width of the sample is comparable with, or smaller than, the bulk mean free path length. On the other hand, if the energy surfaces are spherical, and if carriers are specularly reflected at the boundaries, the electrical conductivity should be independent of the sample width. An investigation of size effects on the electrical conductivity in single crystals requires measurements to be carried out at low temperatures, since it is only then that the mean free path can exceed the minimum width of specimen that can be achieved experimentally. For electrons in bismuth the bulk mean free path is of the order of 1 mm at liquid helium temperature.

For a conductor with non-spherical energy surfaces, such as bismuth, there should be a size effect even if the surface scattering is specular (Price 1960). The electrical conductivity should fall from its bulk value, as the width of specimen is reduced, until it reaches some limiting value which depends on the shape of the energy surfaces and on the orientation of the current flow with respect to the crystal axes. Figure 8 shows the results obtained by Friedman and Koenig (1960) for very high purity bismuth $(\rho_{3000}/\rho_{4\cdot20^\circ}>400)$ at $4\cdot2^\circ\kappa$. The sample was oriented so that the current flow was parallel to a binary axis and the thickness measurement refers to a bisectrix direction. The results were obtained by successively electropolishing the sample to reduce its thickness. The data are consistent with Price's theory assuming the surface scattering to be specular. It is noteworthy that Friedman and Koenig were unable to change the nature of their results by etching the crystals to produce a matt surface or by mechanically abrading the surface.

There are good reasons for supposing that specular reflection is the rule for semi-metals and semiconductors. These reasons are based on the fact that in these materials electron wavelengths are much larger than in metals and are actually comparable with optical wavelengths. Thus, one would at least expect any surfaces that appeared to be specular to visible light to be specular to these long-wavelengths electrons.

An unsatisfactory feature of the experiments carried out by Friedman and Koenig is the fact that they had to remove the sample from the liquid helium for re-etching in between successive measurements. There was



Dependence of electrical conductivity on sample thickness for bismuth at $4\cdot2^{\circ}\kappa$.

thus some possibility of altering the bulk properties by introducing strains during an experiment. For this reason, Aubrey et al. (1964) carried out size-effect measurements using wedge-shaped crystals to which a number of potential leads were attached. As fig. 8 shows, there is a considerable divergence between the results obtained by Aubrey and his colleagues from those of Friedman and Koenig. Aubrey's results display a much greater difference between the bulk conductivity and the thin-sample conductivity, though they also indicate that the conductivity reaches a limiting value for very small widths.

Aubrey et al. discuss their results in terms of a reflectance coefficient p which is equal to unity under some conditions (otherwise the conductivity would fall to zero for a sample of infinitesimal thickness) and less than unity under other conditions. p may, for example, be dependent on both the electron wavelength and on the angle of incidence to the surface. simple approach to this problem it is assumed that p=1 when the change in amplitude Δk of the wavevector on specular reflection is less than some value Δk_0 , whereas if Δk becomes greater than Δk_0 completely diffuse scattering (p=0) is assumed. If it is supposed that $\Delta k_0 = 1.3 \times 10^5 \,\mathrm{cm}^{-1}$, the difference between the bulk conductivity and thin-sample conductivities as measured by Aubrey, can be explained, though the variation with thickness, when the mean free path is comparable with the sample width, is not correctly predicted. However, in view of the disagreement between the two sets of experimental data, it seems important to establish the true variation of the conductivity with thickness for several orientations before further refining the theory.

§ 4. GALVANOMAGNETIC EFFECTS

4.1. Determination of the Effective Mass Tensor

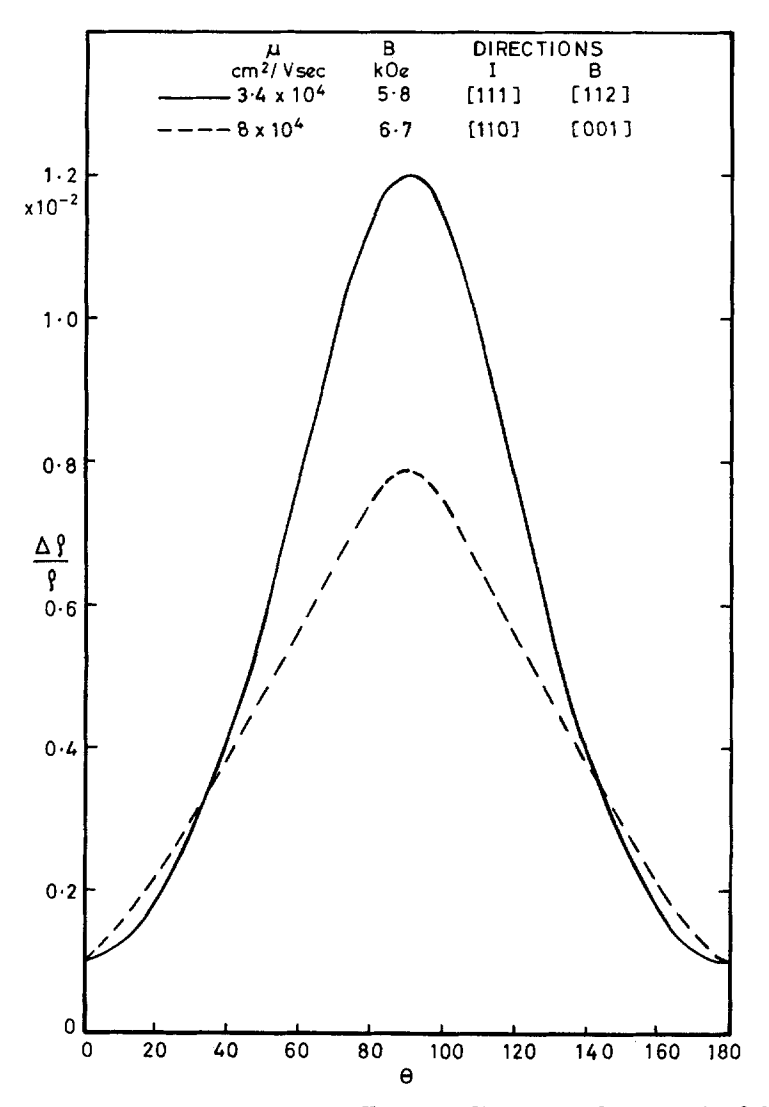
The most direct way of determining the effective mass tensor of a semimetal or semiconductor is by means of one of the cyclotron resonance techniques. However, this requires that the product $\omega_c \tau$ should be at least of the order of unity, ω_c being the cyclotron frequency and τ the relaxation time of the carriers. Even at low temperatures, the relaxation time is high enough to allow eyclotron resonance to be observed in only a few materials. Far more widely applicable is the method of determining the effective mass tensor from the galvanomagnetic coefficients. coefficients are usually measured in magnetic fields that are low enough for the relations between current and electric field to contain terms up to only the second order in B. Having measured the coefficients, it is necessary to select a model for the band structure that is consistent with the experimental data and which is, of course, also consistent with the crystal The method has been described by Abeles and Meiboom (1956) with specific reference to bismuth, by Drabble and Wolfe (1956) for Bi₂Te₃, and by Freedman and Juretschke (1961) for antimony.

Before discussing the galvanomagnetic effects in detail it is worth mentioning that some of the general characteristics can be deduced from relatively simple measurements. Thus, in a cubic crystal the electrical conductivity and Hall coefficient are isotropic but, unless the energy surfaces are centred at $\mathbf{k}=0$ and are, therefore, spherical, the magnetoresistance effects depend on the direction of current flow. A particularly valuable test of whether a material is single-or multi-valleyed is a comparison of the longitudinal and transverse magnetoresistance effects. If the longitudinal magnetoresistance is negligible it can usually be assumed that the surfaces of constant energy are centred at $\mathbf{k}=0$. Figure 9 shows

how the magnetoresistance of n-type HgSe depends on the angle between the current flow and the magnetic field. Since the longitudinal magnetoresistance is so small one can deduce that HgSe has a single-valley conduction band.

It is instructive to consider the galvanomagnetic coefficients for the crystals of the class 3m which include so many of the materials within the scope of this article. For these crystals there are twelve independent

Fig. 9



Dependence of magnetoresistance effect on direction of magnetic field for n-type HgSe (Harman 1961). $\Delta \rho/\rho$ is the magnetoresistance and θ is the angle between the current and magnetic field directions.

coefficients at low magnetic fields. These twelve coefficients are included in the expressions which define the resistivity, Hall coefficient and magnetoresistivity tensors, that is the equations that give the electric field \mathcal{E} in terms of the electric current \mathbf{i} and magnetic field \mathbf{B} :

the other ratios \mathcal{E}_k/i_l being given by the Onsager relation

$$(\mathscr{E}_k/i_l)(B) = (\mathscr{E}_l/i_k)(-B).$$

 ρ_{kl} is the resistivity tensor, ρ_{klm} the Hall tensor and ρ_{kimn} the magnetoresistivity tensor. The directions 1, 2 and 3 refer to the binary axis, bisectrix axis and trigonal axis respectively.

The coefficients defined above can be found by measuring the components of the electric field in selected directions for various directions of current flow and magnetic field. However, certain precautions must be taken if the results are to be accurate. For example, it is important that there are no temperature gradients that could lead to thermoelectric voltages. Such spurious voltages can be avoided by immersing the sample in a liquid bath or by periodically reversing the direction of the electric current, thereby eliminating temperature gradients due to the Peltier effect as well as to any assymetry of the apparatus. The sample should be at least four times as long as it is wide and any measuring probes should be inset by at least the width of the sample from its ends (Drabble and Wolfe 1957); this prevents the ends of the sample from short-circuiting the transverse field over the region on which measurements are made. Furthermore the experiments should be performed at different magnetic field strengths to ensure that terms higher than the second order in B can be neglected (otherwise eqn. (22) is inadequate to describe the results).

The choice of orientation of the samples differs from one worker to another. Thus, Drabble and his colleagues confined their experiments to current flows along the principal crystal axes, rotating the magnetic field in a plane containing the direction of i. Epstein and Juretschke (1963) obtained their results on antimony using two sample orientations with current flow along the trigonal direction and perpendicular to this direction respectively. In the latter case the current flow was set at an angle of 15° to a binary axis rather than along a binary or bisectrix direction in order that all the coefficients could be determined. For both orientations the magnetic field was rotated in a plane containing the trigonal axis. Although, it is not necessary to determine the relation

between electric field and current for all magnetic field orientations, it is wise to do so in order to check that the phenomenological equations are obeyed. Any departure from the phenomenological relations may reveal that the sample is non-uniform or cracked.

Having determined the galvanomagnetic coefficients, these must then be related to the band parameters. The number of independent parameters depends on the model that is adopted. It will be supposed that the material is degenerate (or the relaxation time energy-independent) so that all the carriers in a band have the same relaxation time. It is customary to assume that the bands are parabolic and that the equal-energy surfaces are ellipsoids that are tilted through arbitrary angles with respect to the crystal axes, the parameters at one's disposal being set by the position of the ellipsoids in the Brillouin zone. Thus, if the energy surfaces are centred on the trigonal axis, they must be spheroidal and non-tilted. The simplest model that leads to twelve non-vanishing galvanomagnetic coefficients consists of six ellipsoids centred on the reflection planes and tilted about the binary axes (or three ellipsoids if they are centred at the face of the Brillouin zone). In this situation the parameters that define the galvanomagnetic coefficients for a single band are the carrier concentration n, the mobilities μ_1 , μ_2 and μ_3 along the axes of each ellipsoid, and the angle of tilt ψ between the 3 axis of an ellipsoid and the trigonal (3) axis in the Brillouin zone. For an intrinsic conductor in which only two bands are involved the five variables are increased to nine, whereas for a doped semi-metal, in which the minority carriers cannot be neglected, there are ten variables. These variables can, then, generally be evaluated using less than the complete set of twelve galvanomagnetic coefficients but it is always preferable to make sure that a given solution fits all twelve coefficients, otherwise there is little to justify the adoption of the particular model that has been selected.

In calculating the band parameters it is more convenient to deal with the conductivity coefficients, that occur in the equation for the components of i in terms of & rather than the resistivity coefficients defined by eqn. The equations relating to components of the resistivity tensors to the components of the conductivity tensors have been given by Beer (1963). They are:

$$\rho_{11} = 1/\sigma_{11}, \qquad \rho_{1122} = -\sigma_{1122}/\sigma_{11}^2 - \sigma_{231}^2/\sigma_{11}^2\sigma_{33},$$

$$\rho_{33} = 1/\sigma_{33}, \qquad \rho_{1133} = -\sigma_{1133}/\sigma_{11}^2 - \sigma_{123}^2/\sigma_{11}^3,$$

$$\rho_{123} = -\sigma_{123}/\sigma_{11}^2, \qquad \rho_{1123} = -\sigma_{1123}/\sigma_{11}^2,$$

$$\rho_{231} = -\sigma_{231}/\sigma_{11}\sigma_{33}, \qquad \rho_{3311} = -\sigma_{3311}/\sigma_{33}^2 - \sigma_{231}^2/\sigma_{11}\sigma_{33}^2,$$

$$\rho_{1111} = -\sigma_{1111}/\sigma_{11}^2, \qquad \rho_{2311} = -\sigma_{2311}/\sigma_{11}\sigma_{33},$$

$$\rho_{3333} = -\sigma_{3333}/\sigma_{33}^2, \qquad \rho_{2323} = -\sigma_{2323}/\sigma_{11}\sigma_{33} + \frac{1}{2}\sigma_{123}\sigma_{231}/\sigma_{11}^2\sigma_{33}.$$

$$(23)$$

In these equations the coefficients of ρ and σ are interchangeable.

The expressions for the conductivity coefficients (see, for example, Epstein and Juretschke 1963) are:

$$\begin{split} &2\sigma_{11}=ne[\mu_{1}+c^{2}\mu_{2}+s^{2}\mu_{3}],\\ &\sigma_{33}=ne[s^{2}\mu_{2}+c^{2}\mu_{3}],\\ &-2\sigma_{231}=\pm ne[\mu_{2}\mu_{3}+\mu_{1}(s^{2}\mu_{2}+c^{2}\mu_{3})],\\ &-\sigma_{123}=\pm ne[\mu_{1}(c^{2}\mu_{2}+s^{2}\mu_{3})],\\ &-2\sigma_{1133}=ne[\mu_{1}+c^{2}\mu_{2}+s^{2}\mu_{3}][\mu_{1}(c^{2}\mu_{2}+s^{2}\mu_{3})],\\ &-2\sigma_{3311}=ne[s^{2}\mu_{2}+c^{2}\mu_{3}][\mu_{2}\mu_{3}+\mu_{1}(s^{2}\mu_{2}+c^{2}\mu_{3})],\\ &-3\sigma_{1122}+\sigma_{1111}+2\sigma_{2323}=ne[\mu_{1}+c^{2}\mu_{2}+s^{2}\mu_{3}][\mu_{2}\mu_{3}+\mu_{1}(s^{2}\mu_{2}+c^{2}\mu_{3})],\\ &2\sigma_{2323}=ne[s^{2}\mu_{2}+c^{2}\mu_{3}][\mu_{1}(c^{2}\mu_{2}+s^{2}\mu_{3})],\\ &-2\sigma_{3333}=\sigma_{1122}-3\sigma_{1111}+2\sigma_{2323}=2nec^{2}s^{2}\mu_{1}(\mu_{2}-\mu_{3})^{2},\\ &-4\sigma_{1123}=necs\mu_{1}(\mu_{2}-\mu_{3})[-\mu_{1}+c^{2}\mu_{2}+s^{2}\mu_{3}],\\ &-4\sigma_{2311}=necs(\mu_{2}-\mu_{3})[\mu_{2}\mu_{3}-\mu_{1}(s^{2}\mu_{2}+c^{2}\mu_{3})], \end{split}$$

where c and s are the cosine and sine of the angle of tilt ψ . In the equations for the inverse Hall coefficients, σ_{231} and σ_{123} , the upper sign refers to a hole band and the lower sign to an electron band. We note that for a two-band conductor the contributions from the n_e electrons and the n_h holes are added, so that:

$$2\sigma_{11} = n_{e}e[\mu_{1} + c_{e}^{2}\mu_{2} + s_{e}^{2}\mu_{3}] + n_{h}e[\nu_{1} + c_{h}^{2}\nu_{2} + s_{h}^{2}\nu_{3}],$$

$$-2\sigma_{231} - n_{e}e[\mu_{2}\mu_{3} + \mu_{1}(s_{e}^{2}\mu_{2} + c_{e}^{2}\mu_{3})] + n_{h}e[\nu_{2}\nu_{3} + \nu_{1}(s_{h}^{2}\nu_{2} + c_{h}^{2}\nu_{3})], \text{ etc.,}$$

$$(25)$$

where the μ 's and ν 's are electron and hole mobilities respectively.

In a real experiment one can hardly expect any given set of variables to fit all the observed coefficients exactly. In view of the mass of information and the complexity of the equations, one programmes a computer so that it finds a set of band parameters (or a number of such sets) that are reasonably consistent with the data. It can happen that some of these sets will differ in detail quite considerably; such was the case, for example, in the evaluation of the conduction band parameters for antimony by Epstein and Juretschke though the valence band structure was more or less uniquely determined. It is probably better to work, if possible, with extrinsic rather than intrinsic material, the number of variables then being considerably reduced.

The galvanomagnetic measurements do not determine the effective mass tensor as such, but the effective mass components within a valley are given by the relations $m_1 = e\tau_1/\mu_1$, etc. If the relaxation time τ is isotropic, the ratios of the mobilities along the principal axes of each ellipsoid are the same as the ratios of the reciprocal effective masses. The absolute values of the effective masses cannot be obtained from the galvanomagnetic data on their own. It is necessary, in addition, to know the

Fermi energy, which can be found from Seebeck effect measurements provided that the energy dependence of the relaxation time is known.

An example of the combination of thermoelectric and galvanomagnetic measurements is to be found in the work of Smith, Wolfe and Haszko (1964) on bismuth. Their assumptions of a non-parabolic conduction band with an energy-wavevector relation of the form of eqn. (2) involved the introduction of an additional variable, the direct energy gap $E_{\rm G}$.

If the six-valley tilted ellipsoid model described above has been established already, the shape and tilt of the ellipsoids can be found from three anisotropy ratios, namely the resistivity ratio ρ_{33}/ρ_{11} , the Hall coefficient ratio ρ_{231}/ρ_{123} and a magnetoresistance ratio ρ_{1111}/ρ_{3333} (Drabble 1963). For an extrinsic material with an isotropic relaxation time, the mass ratios and the tilt are given by:

$$\frac{\rho_{33}}{\rho_{11}} = \frac{1+K}{2L},$$

$$\frac{\rho_{231}}{\rho_{123}} = \frac{(M+L)(1+K)}{4KL},$$

$$\frac{\rho_{1111}}{\rho_{3333}} = \frac{L^2(3KL+L+KM-5M)}{2(1+K)^2(KL-M)},$$
(26)

where
$$K=c^2\frac{m_1}{m_2}+s^2\frac{m_1}{m_3}\,,$$

$$L=s^2\frac{m_1}{m_2}+c^2\frac{m_1}{m_3}\,,$$
 and
$$M=\frac{m_1^2}{m_2m_3}\,.$$

These expressions are useful if, for example, one wishes to find out how the band parameters change when one element or compound is added to an isomorphous material (whose band structure is known) so as to form a range of solid solutions.

4.2. Oscillatory Magnetoresistance

When the magnetic field is large $(\mu B \gg 1)$ the classical theory suggests that the electrical conductivity should vary as $1/B^2$ (though the magnetoresistance would be expected to saturate at a relatively low value for an extrinsic conductor). This is the behaviour that is actually observed at ordinary temperatures but at very low temperatures one frequently observes oscillations in the magnetoresistance, the so-called Shubnikov—

de Haas effect, which was, in fact, first seen for bismuth in 1930. Similar oscillations can be seen for transport properties other than the magnetoresistance, as well as for non-transport properties that depend on the charge carriers.

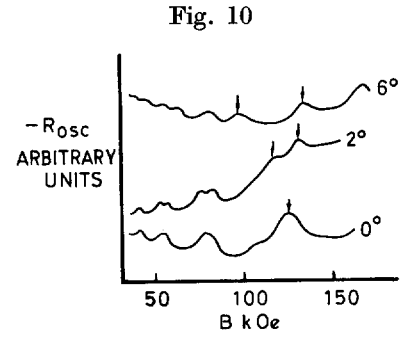
The origin of these oscillatory effects is to be found in the modification of the density-of-states function on the application of a magnetic field. A magnetic field B_z causes the energy of a free electron to be quantized into a series of bands (the Landau bands) such that:

$$E_{n,k_z} = (n + \frac{1}{2})\hbar\omega_c + \frac{\hbar^2 k_z^2}{2m}, \quad . \quad . \quad . \quad . \quad (28)$$

where ω_c is the cyclotron frequency and n the quantum number. The density of states at the Fermi surface becomes infinite if the Fermi energy $E_{\rm F}$, given by $(\zeta - E_c)$ or $(E_v - \zeta)$, is equal to $(n + \frac{1}{2})\hbar\omega_c$. Within the effective mass approximation, this condition is:

$$n + \frac{1}{2} = E_{\rm F} m^* / eB\hbar$$
. (29)

The oscillations are thus periodic in 1/B and the period determines the product of Fermi energy and effective mass.



The oscillatory component of the transverse magnetoresistance plotted against magnetic field for bismuth at $1\cdot2^\circ\kappa$ according to Vuillemin (1964). The angle of tilt of the magnetic field in the binary-trigonal plane, away from the binary axis, is indicated on the right-hand side of each plot.

Certain conditions must be met before oscillations in the magnetoresistance can be observed. In the first place the relaxation time must be appreciably greater than the time for an electron in cyclotron motion to complete an orbit. This condition, $\omega_c \tau \gg 1$, is essentially the same as the high magnetic field condition, $\mu B \gg 1$. It is necessary that the Fermi energy should be much greater than kT and, also, that it should be greater than $\hbar \omega_c$.

Magnetoresistance oscillations due to the electrons in bismuth have, of course, been studied many times since their first observation by Shubnikov and de Haas. In several recent papers study of the oscillations due to holes has been made (Suzuki et al. 1964, Smith, Baraff and Rowell 1964)

and Vuillemin 1964). Strictly, the second term on the right-hand side of eqn. (28) should be written as $\frac{1}{2}s\hbar\omega_s$ where s is the spin quantum number and $\omega_s = eB/m_s$, m_s being the spin mass defined by 2m/g and g being the effective g-factor. Particular attention has been drawn to the spinsplitting of the hole oscillations by Smith and his colleagues and by Vuillemin. Vuillemin's observations of the spin splitting, as the magnetic field is rotated away from the binary axis for bismuth at 1.2°k, are illustrated in fig. 10.

The conditions for the observation of magnetoresistance oscillations can be satisfied for several other semi-metals and narrow-gap semiconductors besides bismuth, at liquid helium temperatures. For example, they have been studied in p-type Bi₂Te₃ at $4\cdot 2^{\circ}$ k by Landwehr and Drath (1964) using pulsed fields of up to 185 koe. These workers were not able to use a sufficient number of different orientations to allow a completely independent determination of the effective mass tensor, but their results were consistent with the band structure obtained from low-field galvanomagnetic measurements at 77°K.

§ 5. Non-linear Effects

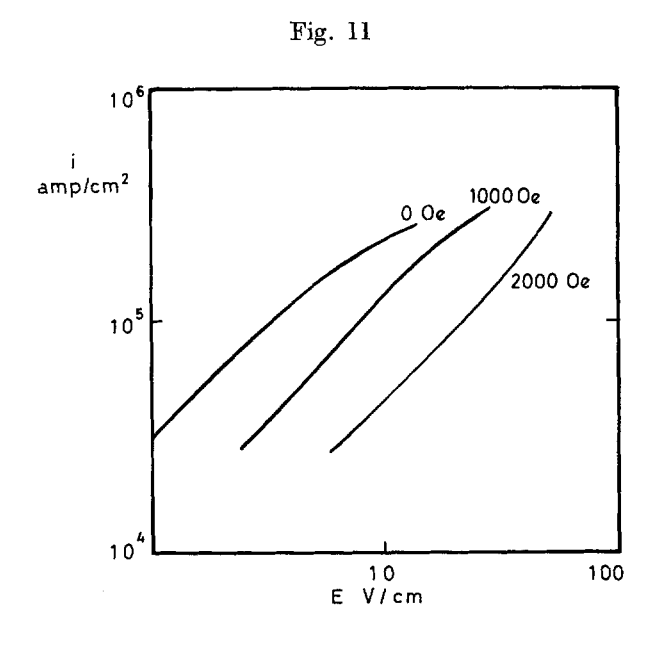
5.1. Self-magnetic Field and Diffusion Effects

In their measurements of the current-voltage characteristics of bismuth at 77°k, Hattori and Steele (1963) found an apparent increase in the resistivity for high electric fields. This phenomenon can be attributed to magnetoresistance arising from the self-magnetic field induced by a large electric current. Later, Hattori and Tosima (1956) found that, when a transverse magnetic field of more than a certain strength was applied, the resistivity appeared to decrease at high electric fields. Hattori and Tosima's results are shown in fig. 11. The dimensions of the sample were about 0.04 cm, 0.004 cm and 0.5 cm in the binary, bisectrix and trigonal directions respectively. The current flow was along the trigonal direction and the magnetic field lay parallel to a bisectrix axis. Samples with other orientations have also been studied.

Hattori and Tosima's observations can be explained qualitatively in terms of the simple Abeles and Meiboom band model. Briefly, the change in the current-field characteristic from sublinear to superlinear form, on increasing the externally applied magnetic field, is due to two Firstly, the self-magnetic field and the applied field are additive over one-half of the cross section whereas they oppose one another over the other half. It is found that the increased magnetoresistance when the fields act together is insufficient to compensate for the decreased magnetoresistance when they act in opposition. Secondly, the combination of self and applied fields leads to a resultant that has a component along the binary axis, leading to only a weak magnetoresistance effect, whereas, if there were no self field, the magnetic field would lie wholly along the bisectrix axis, this producing the strongest magnetoresistance effect.

Although the above considerations are basically correct they do not give an accurate prediction of the changeover of the characteristic from sublinear to superlinear. Some account should, of course, be taken of such phenomena as self-pinching but it is believed that the primary reason for the inadequacy of the simple theory lies in a size effect associated with carrier diffusion. A diffusion-size effect has been demonstrated for bismuth, also at 77°k, by the same authors (Tosima and Hattori 1964).

In experiments on the magnetoresistance and Hall effect (at low electric fields, so that the possibility of self-magnetic field effects can be ignored) Tosima and Hattori found substantial deviations from Abeles and Meiboom's (1956) results when the thickness of the sample was less than 0.01 cm. Now the mean free path of the carriers at 77°K is of the order of 10⁻⁴cm, so this cannot be the ordinary size effect which appears when the sample dimensions approach the free path length. Instead, it must be assumed that the inter-valley relaxation times are long enough for appreciable non-equilibrium carrier populations to be built up by diffusion processes. If the electron-hole relaxation time is long there can be a build-up of nonequilibrium electron-hole pairs. Also, in view of the fact that the applied magnetic field and the current flow cannot be parallel to principal axes for more than one of the three electron ellipsoids, there can be an exchange of electrons between the other two ellipsoids, if the appropriate relaxation time is long enough. The experiments are consistent with inter-valley relaxation times (or lifetimes) of the order of 10⁻⁹ sec.



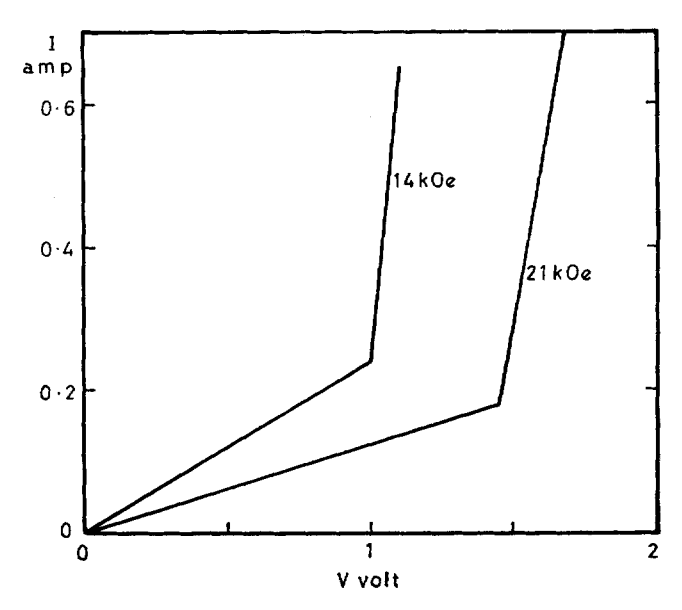
Self-magnetic field effect in bismuth at 77°k. Plot of current against electric field for different transverse magnetic fields (Hattori and Tosima 1965).

Very much larger carrier lifetimes are expected at liquid helium temperature (Esaki 1962 a). In this connection it is interesting to note the observation by Zitter (1965) of the photoelectromagnetic (PEM) effect in bismuth at 4.2°K. It will be recalled that this effect, which is of importance in determining carrier lifetimes in semiconductors, consists of the separation of diffusing electron-hole pairs by means of a transverse magnetic field. It is difficult to observe in a semi-metal because of its very low electrical impedance, but Zitter was able to match the impedance of the amplifier to that of his sample by using a superconducting transformer. that the time for recombination of electron-hole pairs is about 10⁻⁸ sec, which is an order of magnitude larger than the intra-valley relaxation time at the same temperature. . In other words, inter-valley scattering is much less effective than intra-valley scattering in a semi-metal, where it requires a change of momentum but no change of energy, just as it is in a semiconductor, where, of course, it requires a change of energy as well.

5.2. Esaki Kink Effect

A non-linear current-voltage characteristic of a different kind was first observed by Esaki (1962 a, b) when he was making magnetoresistance measurements on bismuth at liquid helium temperatures. Some typical experimental results are shown in fig. 12 for a single crystal at 2°K with current flow along the bisector between the binary and bisectrix axes and the magnetic field along the trigonal axis. The cross section of the sample was about 1 mm².

Fig. 12



Current-voltage characteristics for a sample of bismuth in magnetic fields of 14 and 21 koe at 2°K (Esaki 1962 a).

A.P.

Ohm's law is obeyed until the electric field reaches a critical value (the kink field) beyond which the differential resistance becomes very much smaller. The change of slope at the kink field is the more marked, the higher the transverse magnetic field.

A key to the explanation of the phenomenon is the fact that the electric field at the kink is proportional to the magnetic field strength for a given orientation, the constant of the proportionality being about $10^{-3} \,\mathrm{v/cm}$ oe. As Esaki pointed out, the combination of an electric field $\mathscr E$ with a crossed magnetic field B leads to a drift of carriers in the mutually perpendicular direction with a velocity v given by:

$$v = \frac{\mathscr{E}}{B}. \qquad . \qquad (30)$$

Thus, the kink is observed at a constant drift velocity of about 10^5 cm/sec which is close to the appropriate velocity of sound in bismuth. This suggests that the effect is due to an enhanced interaction between the charge carriers and the phonons when the drift velocity of the former reaches the speed of propagation of the latter. The corresponding increase in the scattering probability reduces the mobility of the carriers and thereby increases the conductivity in the presence of the strong magnetic field (the strong-field electrical conductivity is proportional to $1/\mu B^2$).

Pippard (1963) has discussed the enhanced electron-phonon interaction in semiconductors and semi-metals, when the carrier drift velocity exceeds the sound velocity, in terms of stimulated emission arising from population He has pointed out the equivalence of a quantum treatment (as used by Esaki) and a treatment in terms of a classical bunching process (Hopfield 1962). Pippard considered specifically the simple example of a conductor with spherical surfaces of constant energy and showed that, if both energy and momentum are to be conserved in an electron-phonon interaction, there must be a planar surface of interaction (in k space) given by $\hbar k_x = m^*u$, where x is the direction of sound propagation and u is the velocity of sound. The probabilities of absorption and emission of phonons differ in the value of the factor $f_1(1-f_2)$, where f_1 and f_2 are the occupation probabilities of the initial and final electron states. When the electron gas is in equilibrium, this factor must increase with amplitude of the electron wavenumber so that phonon absorption is the more probable, but when a current is flowing the centre of the distribution function is shifted away from $\mathbf{k} = 0$ and it is possible for $f_1(1 - f_2)$ to become greater for emission rather than absorption of phonons. The required population inversion occurs when the drift velocity exceeds the velocity of sound.

Amplification of sound waves in the direction of a strong electric field is now familiar in CdS (Hutson et al. 1961). Such a field can be applied to CdS without excessive heating because the electrical conductivity is very small; the strong piezo-electric coupling between the electrons and phonons is also an advantage. In most other semiconductors the electrical conductivity is so high that intense heating of the sample occurs when

it is subjected to a high electric field. On the other hand, the higher the carrier concentration, the more marked should be the effect if it can be made to occur. The very high electrical conductivity of the semi-metals, of course, rules out ultrasonic amplification under the influence of an electric field alone. However, when a strong transverse magnetic field is also applied the magnetoresistance effect leads to a very considerable reduction in the power dissipation for a given electric field. that the conductor should be intrinsic and that both electrons and holes have a high mobility, otherwise the Hall field will reduce the magnetoresistance effect. This condition is met in pure bismuth and accounts for the success of Esaki's experiment.

The Esaki kink effect and its explanation suggest that ultrasonic amplification in a transverse direction should be possible in a sample of bismuth that is subjected to crossed electric amd magnetic fields. effect has been observed by Toxen and Tansal (1963) who reported sound amplification of up to 14 dB/cm at a frequency of 14 Mc/sec.

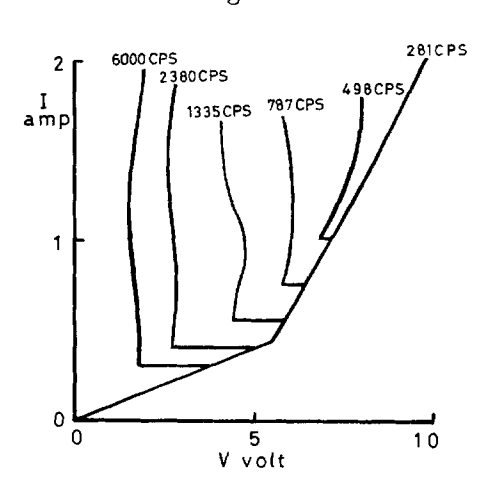


Fig. 13

Pulsed current transverse magnetoresistance of bismuth in liquid helium. For experimental details see Goldsmid and Corsan (1964).

It will be appreciated that the Esaki effect is rather difficult to demonstrate even in bismuth, and conditions are certainly less favourable for the other Magnetoresistance experiments on antimony and arsenic have, however, also yielded a kink effect at liquid helium temperature, though this effect is of thermal origin (Eastman and Datars 1963). effect manifests itself as a sudden fall in the electrical resistance at a constant current, when the electric field reaches a critical value. Further increase in the current leads to a gradual decrease in the electric field. The critical electric field is proportional to the transverse magnetic field just as for the true Esaki effect. The phenomenon can be explained by the sudden onset on film boiling of the liquid helium in contact with the sample, when the rate of heat dissipation at the surface exceeds a certain value. The relatively poor heat transfer under film-boiling conditions implies that the temperature of the sample must rise considerably, the mobility then falling and the conductivity (in a given magnetic field) becoming larger.

The Esaki effect and the thermal kink effect have been observed on the same sample by Goldsmid and Corsan (1964) whose results are given in fig. 13. The sample of bismuth was subjected to short pulses of fixed duration but of variable repetition rate. When the pulse repetition frequency was low the Esaki kink was clearly seen but as the repetition frequency was increased the power to be dissipated became greater and the thermal kink appeared, so preventing the drift velocity of the carriers from reaching the sound velocity. In the same set of experiments the Esaki effect was also observed for a sample of reheated pyrolytic graphite.

§ 6. Thermomagnetic Effects

6.1. Nernst and Ettingshausen Effects

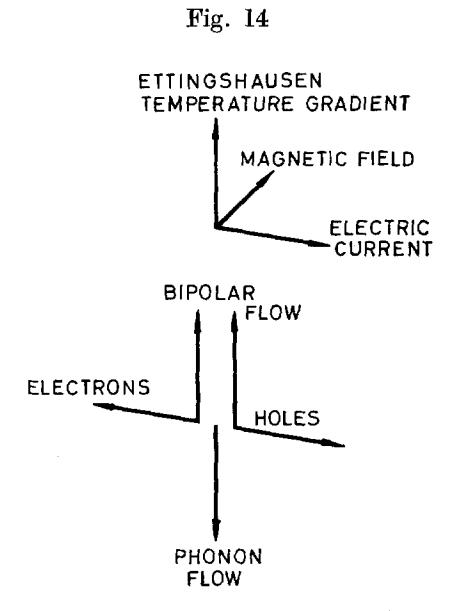
Some of the most remarkable of the transport properties of semi-metals are to be found among the thermomagnetic phenomena. As we shall see the conditions for the observation of some of these effects can be more favourable for the intrinsic semi-metals than for any other class of material. However, first let us consider the origin of the Nernst and Ettingshausen effects in an extrinsic conductor. The Nernst and Ettingshausen coefficients, Q and P, are related to one another by Bridgman's equation:

$$P\kappa = QT, \qquad (31)$$

which may be compared with Kelvin's relation between the Seebeck and Peltier coefficients. It suffices, then, to discuss the origin of one of the other of the effects; here the Ettingshausen effect is chosen, though the Nernst coefficient is usually the easier to determine experimentally.

The interaction of a transverse magnetic field with a longitudinal current flow does not lead to a transverse electric current under the customary conditions of measurement; this is because the field due to the Lorentz force is balanced by the Hall field. If there were no transverse movement of the charge carriers whatever, there could be no transverse heat transfer and, therefore, no Ettingshausen effect. There are, however, partial flows of the carriers of different energy if the relaxation time is energy-dependent. The Nernst and Ettingshausen effects, thus, depend for their sign and magnitude on the energy dependence of the relaxation time and can be used, in principle, to determine the scattering law, provided that the density-of-states function is known. According to the usual conventions P and Q have the same sign as the exponent λ in the scattering law. Care must be taken, however, if optical-mode scattering is thought to be predominant, since a scattering law of the form of eqn. (4) is not then

usually applicable (Ehrenreich 1961). It should be noted that the Nernst and Ettingshausen coefficients tend to zero for high magnetic fields; a high magnetic field $(\mu B \gg 1)$ has the effect of eliminating any phenomena that depend on differences of relaxation time between the carriers (Tsidil'kovskii 1962).



Origin of the Ettingshausen effect in an intrinsic conductor.

Valuable though the low field transverse thermomagnetic effects can be in determining the scattering law for an extrinsic conductor, the effects are much larger for an intrinsic conductor. This can be explained with reference to fig. 14 which shows the origin of the Ettingshausen effect when there are equal numbers of electrons and holes. The longitudinal current flow results from the electrons and holes moving in opposite directions, but the magnetic field causes both types of carrier to move If the carriers have the same mobility in the same transverse direction. there will be no Hall field since the partial current flows are then equal and opposite to one another. In effect, electron-hole pairs are generated at one face of the sample and annihilated at the opposite face, thus transferring their ionization energy from one side to the other. This lateral bipolar flow sets up a temperature gradient so that, in equilibrium, it is balanced by conduction of heat in the opposite direction. The transverse thermomagnetic coefficients associated with the bipolar effect are generally larger than for a single type of carrier and, moreover, remain large at high magnetic field strengths. The bipolar Nernst and Ettingshausen coefficients are always positive in sign.

There is an interesting relationship between the high-field Nernst coefficient and the high-field magnetoconductivity for any intrinsic conductor, as was first pointed out by Kooi $et\ al.$ (1963). Suppose that we have multi-valley valence and conduction bands. Then, for the carriers in valley l the currents in the x and y directions are:

$$i_{x}(l) = \sigma_{x}(l) \left[\mathscr{E}_{x} - \alpha(l) \frac{dT}{dx} - R(l)Bi_{y}(l) \right],$$

$$i_{y}(l) = \sigma_{y}(l) \left[\mathscr{E}_{y} - \alpha(l) \frac{dT}{dy} + R(l)Bi_{x}(l) \right],$$
(32)

the magnetic field B being in the z direction. $\alpha(l)$ and R(l) are the partial Seebeck coefficient and Hall coefficient that are appropriate to the carriers within the valley l and $\sigma_x(l)$ and $\sigma_y(l)$ are the contributions to the electrical conductivity in the x and y directions.

The solution of eqns. (32) for the conditions dT/dx = dT/dy = 0 and the summation of the current contributions $i_x(l)$ due to each valley immediately yields the electrical conductivity in the x direction:

$$\sigma_x(B) = \sum \frac{\sigma_x(l)}{1 + B^2 R^2(l) \sigma_x(l) \sigma_y(l)} . \qquad (33)$$

When the high magnetic field condition applies for all the carriers, eqn. (33) becomes:

$$\sigma_x(B) = \frac{1}{B^2} \sum_{\mu_y(l)} \frac{n(l)e}{\mu_y(l)}, \qquad (33')$$

where n(l) is the number of carriers in valley l and $\mu_{\nu}(l)$ is their mobility in the y direction.

In order to determine the high-field Nernst coefficient Q_{xy} , for a temperature gradient dT/dy leading to an electric field \mathscr{E}_x , one applies the conditions dT/dx=0 and $\sum i_x(l)=\sum i_y(l)=0$. When this is done it is found that, for high magnetic fields:

$$Q_{xy} \equiv \frac{\mathscr{E}_x}{B \, dT / dy} = \frac{n_i e(\alpha_h - \alpha_e)}{\sum n(l) e / \mu_y(l)}, \quad . \quad . \quad . \quad . \quad . \quad (34)$$

where n_i is the total electron or hole concentration. Combining eqns. (33') and (34):

$$Q_{xy} = \frac{n_i e(\alpha_h - \alpha_e)}{B^2 \sigma_x(B)}, \qquad (35)$$

which is the relationship derived by Kooi and his colleagues. In making use of this expression it should be noted that the partial Seebeck coefficients have their high field values which may be rather different from their zero field values. The difference $\alpha_h - \alpha_e$, of course, represents the energy carried by an electron-hole pair (multiplied by 1/eT).

It is instructive to examine eqn. (34) for an isotropic conductor with spherical energy surfaces for both electrons and holes. The expression for the Nernst coefficient at high fields then becomes:

$$Q = \frac{\mu_e \mu_h}{\mu_e + \mu_h} (\alpha_h - \alpha_e). \qquad (36)$$

It is readily seen that the value of the Nernst coefficient is controlled by the smaller of the two carrier mobilities. It is necessary that both types of carrier should have high mobilities if the Nernst coefficient is to be large, just as they should both be highly mobile for a large bipolar contribution to the thermal conductivity.

The Nernst coefficient is little more difficult to measure than the Hall coefficient but the Ettingshausen effect is much harder to observe unless favourable electronic characteristics are combined with a relatively low thermal conductivity. This is indeed the situation for bismuth, which is one of the few materials on which the effect has been studied in any systematic fashion. The Bi-Sb alloys are also favourable for the examination of the Ettingshausen effect since they have lower thermal conductivities than that of pure bismuth.

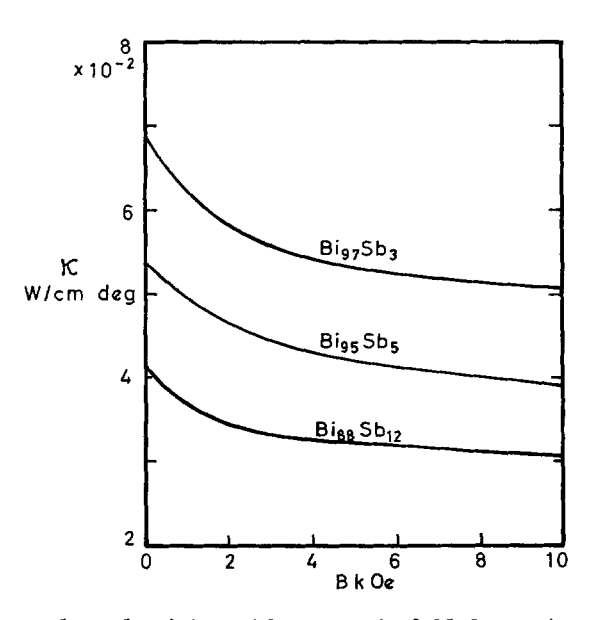
Although the thermomagnetic effects are very easily detected in a material such as bismuth, one major experimental difficulty does arise. The Nernst coefficient of direct theoretical significance is the so-called isothermal coefficient, as defined above for zero transverse temperature In practice, however, one measures the adiabatic coefficient for which the transverse heat flow is zero. The presence of a transverse temperature gradient (due to the Righi-Leduc effect) implies that there must be a transverse thermoelectric voltage between any potential probes that do not have the same Seebeck coefficient as the sample. thermoelectric voltage that leads to the difference between the adiabatic and isothermal Nernst effects and it can be large enough even for the adiabatic and isothermal coefficients to be of opposite sign. any material that has a large Righi-Leduc coefficient, it is important that this quantity (and also the Seebeck coefficient) should be determined at the same time as the adiabatic Nernst coefficient, in order that the isothermal Nernst coefficient can be found.

6.2. Magneto-thermal Resistance

The measurement of the change of thermal conductivity in a magnetic field, or the Maggi-Righi-Leduc effect, is in many instances the most direct way of separating the lattice and electronic components of the thermal conductivity. The electronic part of the thermal conductivity, like the electrical conductivity, can be made vanishingly small by the application of a sufficiently large magnetic field, the remaining heat conductivity being due solely to the lattice. The heat conduction by the lattice vibrations can compensate for any lateral heat transfer by the charge carriers, so that the electronic thermal resistivity in a magnetic field does not reach saturation in the same way as the magnetoresistivity sometimes does.

It is most useful to determine the magneto-thermal resistance effect when the magnetic field is of sufficient strength to reduce the electronic thermal conductivity to a very small fraction of its zero field value. This can certainly be done for bismuth and Bi–Sb alloys with less than about 20% antimony, at liquid nitrogen temperature. Thus fig. 15 shows the effect of a magnetic field of up to 10 koe on three different Bi–Sb alloys at 80°K, according to Kooi et al. (1963). At the highest field the electronic thermal conductivity is so small that the lattice component can be calculated accurately from the data.

Fig. 15



Change of thermal conductivity with magnetic field for various Bi-Sb alloys at 80°κ (Kooi et al. 1963). The temperature gradient lies parallel to a binary axis and the magnetic field is parallel to a bisectrix direction.

At ordinary temperatures the electronic thermal conductivity along the basal planes of graphite is negligible but Klein (1964) and Holland have shown that the electronic component accounts for nearly half the total thermal conductivity at $2^{\circ}\kappa$. They demonstrated this by applying a magnetic field of about 5 koe, reducing the thermal conductivity from 7×10^{-3} w/cm deg to less than 4×10^{-3} w/cm deg. As is expected for a strongly degenerate conductor, the Lorenz number was found to have the value $(\pi^2/3)(k/e)^2$ whatever the applied magnetic field. As mentioned previously, the bipolar contribution to the heat conductivity in graphite is negligible at $2^{\circ}\kappa$.

The magneto-thermal resistance effect can be used for separating the lattice and electronic thermal conductivities, even when the change in the latter on applying a magnetic field is small. In this case, one determines

the ratio of the changes of thermal conductivity and electrical conductivity in a magnetic field for an extrinsic sample, ensuring that the ratio is independent of field strength over the range covered by the experiment. This ratio, like the Seebeck coefficient, is a function of the Fermi energy $E_{\rm F}$ and of the scattering exponent λ so that, if the Seebeck coefficient is also measured, $E_{\rm F}$ and λ can be determined. This in turn allows one to calculate the Lorenz number and hence the electronic thermal conductivity. This approach has been examined for Bi₂Te₃ by Bowley et al. (1958) who found, however, that it was better to determine $E_{\rm F}$ and λ from the magneto-Seebeck effect. The magneto-Seebeck effect, like the Nernst effect, determines λ uniquely whereas the magneto-thermal resistance effect generally yields two possible values for λ .

Before terminating this discussion of the magneto-thermal resistance effect, mention should be made of a particular situation that prevents the thermal conductivity from falling to the value of the lattice component. Strictly speaking, the electronic thermal conductivity only tends to zero in a high magnetic field for an intrinsic conductor if the transverse electric field is zero. If, instead, the transverse electric current is zero, there is a transverse-transverse contribution arising from the Nernst effect acting on the electrical conductivity and the Ettingshausen effect (Delves 1964). In this case the high field thermal conductivity is given by:

where
$$Z_{\rm NE} = \frac{\kappa_{\rm L}(1+Z_{\rm NE}T)}{\kappa_{\rm L}\rho(B),}$$

 κ_{L} being the lattice thermal conductivity. This effect could certainly be of some importance for bismuth and its alloys which have large values of $Z_{\rm NE}$ as will be mentioned later.

6.3. Magneto-Seebeck Effect

It has already been pointed out that the magneto-Seebeck effect in an extrinsic conductor can be used in determining the scattering law. As shown by eqns. (11) and (11') the Seebeck coefficient in zero magnetic field is the sum of one term involving just the Fermi energy and another involving the kinetic energy. The second term is a function of both the Fermi energy and the scattering parameter λ but can be made independent of λ in a high enough field (for the same reason that the Nernst coefficient then disappears). If the conductor is non-degenerate with parabolic bands, the change in Seebeck coefficient is equal to $\pm \lambda(k/e)$ in a high field, the upper sign applying for an n-type conductor and the lower for a p-type conductor. For a partially degenerate conductor the change is somewhat smaller (Tsidil'kovskii 1962) and is a function of the Fermi energy as well as λ .

It is unusual to have a high enough magnetic field available to achieve the saturation value for the Seebeck coefficient, but a measurement of the ratio of change in Seebeck coefficient to change in electrical conductivity at low fields also suffices to determine λ (Bowley et al. 1958).

The magneto-Seebeck effect is more complicated for an intrinsic conductor but, provided that transverse electric fields and temperature gradients are eliminated, the Seebeck coefficient can be calculated using eqn. (19) with the values of $\alpha_{e,h}$ and $\sigma_{e,h}$ appropriate to the magnetic field. The experimental results obtained by Wolfe and Smith (1962) on bismuth and Bi-Sb alloys, are, however, much more interesting than this would suggest.

The Seebeck coefficient of bismuth in zero field is negative since the electrons are more mobile than the holes. On applying a magnetic field, one would expect the partial Seebeck coefficients to rise (assuming the scattering exponent λ to be negative) but the stronger magnetoresistance effect on the electrons than the holes would tend to reduce the overall Seebeck coefficient. One would certainly not expect the magnitude of the Seebeck coefficient to rise by even as much as $-\lambda(k/e)$, i.e. about $40 \,\mu\text{v}/\text{deg}$. Thus, the observation by Wolfe and Smith that the Seebeck coefficient of bismuth in the direction of the trigonal axis can be changed from $-130 \,\mu\text{v}/\text{deg}$ to about $-300 \,\mu\text{v}/\text{deg}$ at $160 \,^{\circ}\text{K}$ with a magnetic field of 5 koe (applied along a bisectrix direction) is, at first, most surprising.

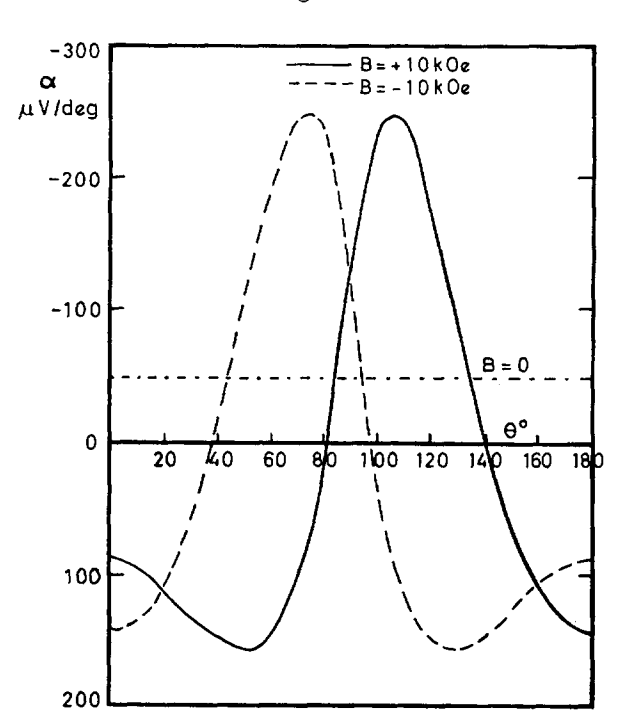
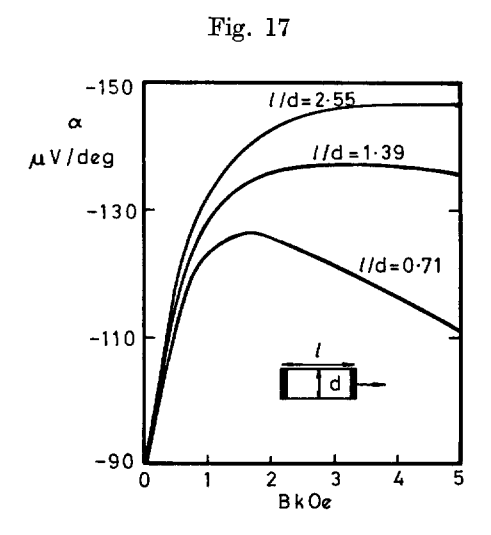


Fig. 16

Orientation dependence of the magneto-Seebeck effect in bismuth at 80° K. The heat flow lies along a bisectrix direction and θ is the angle between the transverse magnetic field and one of the binary axes (Smith, Wolfe and)Haszko 1964).

Equally curious is the observation of a strong 'umkehr' effect for This effect, which can only occur for certain crystal orientations, manifests itself as a difference between the values of the Seebeck coefficient for the same magnetic field in opposite directions, i.e. $\alpha(B) \neq \alpha(-B)$. In fact, one can obtain a positive Seebeck coefficient with the magnetic field in one direction and a negative Seebeck coefficient when its direction is Comprehensive studies of the umkehr effect in bismuth have been reported by Smith, Wolfe and Haszko (1964); some of their results are shown in fig. 16 in which the Seebeck coefficient at 80°k is plotted as a function of the magnetic field orientation for a magnetic field of 10 koe, with the temperature gradient in a bisectrix direction. The umkehr effect cannot occur when the magnetic field lies in a reflection plane (a trigonal-bisectrix plane) but a rotation of the magnetic field to make an angle of only about 20° with the trigonal axis leads to a very strong umkehr effect indeed.



Geometry dependence of the magneto-Seebeck effect in a Bi₉₃ Sb₇ alloy. The heat flow lies along the trigonal axis and the magnetic field along a bisectrix axis (Ertl et al. 1963).

The measurements of Smith and his colleagues were all carried out using long samples with no transverse flows of heat or electricity. It is, therefore, reasonable to suppose that the magneto-Seebeck effects that they observed were strongly influenced by the transverse thermomagnetic phenomena. Longitudinal electric fields can result from the interaction of the Hall and Nernst effects and of the Nernst and Righi-Leduc effects. true that the more striking of Smith's results are due to the transversetransverse effects one would expect them to become less strong for samples of short length, since the electrodes at the end faces act as electrical and thermal short circuits. Figure 17 shows that the increase in Seebeck

coefficient with magnetic field for a Bi-Sb alloy does indeed become smaller as the length-to-width ratio of the sample is reduced, the behaviour being consistent with the measured values of the transverse coefficients (Ertl *et al.* 1963).

6.4. Righi-Leduc Effect

The Righi-Leduc effect is one of the most difficult of the transport phenomena to observe with any degree of accuracy and it does not usually lead to any information that cannot be obtained from the other effects. Where the Righi-Leduc coefficient is determined, this is primarily to provide data for calculating the other parameters under isothermal conditions.

For an extrinsic conductor, the Righi–Leduc angle (the tangent of which is equal to the transverse temperature gradient divided by the longitudinal gradient) is approximately equal to the Hall angle multiplied by the ratio $\kappa_{\rm E}/\kappa$. The Righi–Leduc effect is, then, largest when the electronic thermal conductivity is an appreciable portion of the total. Unlike the Hall angle, the Righi–Leduc angle does not continually increase with magnetic field, since the magneto-thermal resistance effect tends to make the ratio $\kappa_{\rm E}/\kappa$ small for high fields. The author, has, for example, observed a Righi–Leduc angle as large as $\tan^{-1}0.1$ for a sample of $\mathrm{Bi}_{94}\mathrm{Sb}_6$ in a magnetic field of 1 koe at a temperature of 80°K whereas the Righi–Leduc angle was only $\tan^{-1}0.04$ in a field of 8 koe.

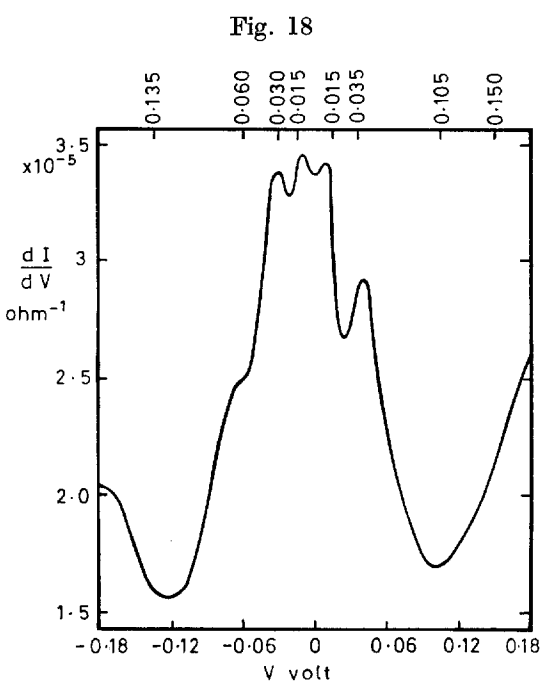
Righi–Leduc measurements have been reported for HgSe by Whitsett (1961), the effect being large in this material because of its high electron mobility and low lattice thermal conductivity. Whitsett observed tangents of the Righi–Leduc angle as high as 0·2 for some of his samples at room temperature. The low-field Righi–Leduc coefficient S at 300°K for a sample containing 6×10^{17} electrons/cm³ was found to be $3\cdot4\times10^3$ cm²/v sec. The electronic thermal conductivity of this sample was calculated to be 6×10^{-3} w/cm deg while the total thermal conductivity was measured as 25×10^{-3} w/cm deg. The value of $S\kappa/\kappa_{\rm E}$ is therefore about $1\cdot4\times10^4$ cm²/v sec which is very close to the predicted value of $7\mu_{\rm H}/8$, the Hall mobility $\mu_{\rm H}$ being equal to $1\cdot5\times10^4$ cm²/v sec.

§ 7. Tunnel Effect

Very recently it has been demonstrated, contrary to predictions, that observations on the tunnelling current between a semi-metal and an insulator can give information about the band structure of the semi-metal that is difficult, if not impossible, to obtain by other methods (Esaki and Stiles 1965). The sample used in the experiments consisted of a film of $\mathrm{Al_2O_3}$ of several tens of angströms thickness, deposited on a cleavage surface of bismuth, with an aluminium counter-electrode of about $10^{-4}\,\mathrm{cm^2}$ area. A plot of dI/dV against V, where I is the current and V is the voltage, is shown in fig. 18, with the fine structure omitted, the results having been obtained at $2^\circ \kappa$.

An analysis of the original curve yields eight components with peaks at the positions indicated in fig. 18. These peaks can be associated with the various band extrema. Thus the peaks at -15 and +15 millivolt correspond to the principal valence band maximum and conduction band minimum respectively. The peak at +35 millivolt is due to the valence band maximum at the same location in the Brillouin zone as the principal conduction band minimum. The other peaks correspond to band extrema that have not previously been identified, though Esaki and Stiles tentatively associate the conduction band that produces the peak at -30 millivolt with the principal valence band, in view of the similar values of the conductance.

As Esaki and Stiles point out, the technique could prove very valuable in future studies, and they suggest that it should be applied to the Bi-Sb alloys.

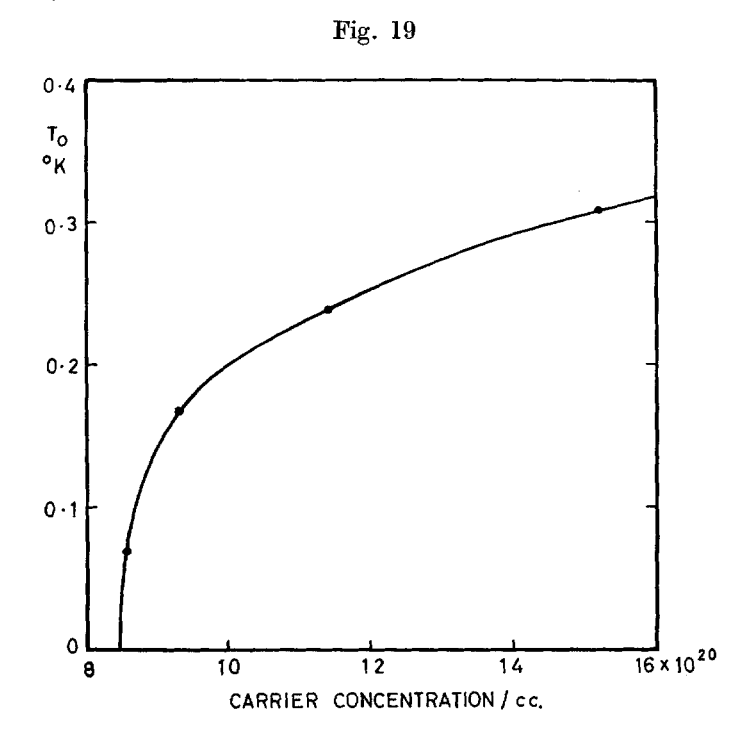


Plot of dI/dV against voltage for a bismuth-Al₂O₃ junction at 2°K (Esaki and Stiles 1965). The fine structure has been omitted.

§ 8. Superconductivity

It is a notable feature of superconductivity that its observation has, until recently, been confined to the true metals rather than semi-metals or semiconductors. It has, in fact, been observed for bismuth (Shoenberg 1938) but only for thin films which have a Hall constant that is much smaller than for the bulk element and must therefore be regarded as metallic rather than semi-metallic (Buckel 1959).

The absence of superconducting behaviour for semiconductors is, of course, completely consistent with the BCS theory (Bardeen et al. 1957) in which one of the criteria for superconductivity is a high density of states at the Fermi surface. Thus, if one is searching for new superconductors, one stands little chance if one looks at materials in which the Fermi surface lies close to the band extrema. On the other hand, the possibility of altering the carrier concentration in semi-metals and semiconductors by doping would make the study of superconductivity in such materials very attractive. As Cohen (1964) has pointed out, semiconductors have a great advantage over metals in that the carrier concentration and band structure can be varied independently of one another by using doping or non-doping impurities.



Plot of superconducting critical temperature against carrier concentration for GeTe (Hein et al. 1964).

Cohen has discussed in some detail the conditions under which superconductivity might appear in a semiconductor or semi-metal. Basically, what is needed is a high carrier concentration and strong electron-phonon coupling. The right conditions are more likely to be found in a multivalley conductor rather than a single-valley material. For a given set of valley parameters, the carrier concentration increases proportionately with the number of valleys. Also, inter-valley electron-phonon processes are more favourable than intra-valley processes since they involve large momentum transfer and are, therefore, relatively unscreened. Screening of the intra-valley repulsive Coulomb interaction due to the large number of carriers is an advantage. A high static dielectric constant, such as is usually found for semi-metals, also assists in screening the Coulomb interaction. Other requirements are a high effective mass within valleys (since this increases the density of states), a high inter-valley coupling constant, and a large phonon degeneracy factor.

Cohen's predictions have been well borne out by Hein et al. (1964) who have discovered that superconductivity can occur in GeTe. GeTe has an effective mass that is almost as high as the free-electron mass and invariably has a large hole concentration which can be adjusted within limits by changing the concentration of germanium vacancies. In the reported experiments the hole concentration lay between 7.5×10^{20} and 15×10^{20} per cm³. The results of Hein et al. are shown in fig. 19. A transition temperature of about 0.3°K was observed for the sample with the highest carrier concentration whereas no superconducting behaviour could be found when there were less than about 8.5×10^{20} holes/cm³. Hein and his colleagues were careful to check the elemental germanium and tellurium, that were used in making the compound, to ensure that there were no traces of superconducting impurities present. It is noteworthy that the critical carrier concentration in GeTe lies close to the empirical limit of 10¹⁹ holes/cm³ proposed by Chapnik (1962) who also suggested that the interatomic spacing should lie between 2.6-2.9 Å and 4 Å if a given material were to be a superconductor.

More recently (Hannay et al. 1965) have observed superconductivity in the so-called intercalation compounds of graphite with the alkali metals, potassium, rubidium and caesium. The highest of the transition temperatures was found for the potassium-graphite compound with the formula C₈K. It will be interesting to see whether the superconducting properties of the graphite compounds fit in with Cohen's ideas as outlined above, or whether they are due essentially to their two-dimensional nature, as Hannay and his colleagues suggest.

§ 9. APPLICATIONS

The transport properties discussed in this article could be utilized in certain practical devices. A full consideration of these devices could, of course, itself occupy a whole article, but a brief mention of the possibilities will no doubt be of interest.

High mobility materials are certainly required for applications of the Hall and magnetoresistance effects. However, Hall elements of low electrical impedance cannot readily be matched to conventional amplifiers, so the high carrier concentration of all the materials mentioned here is a great disadvantage. On the other hand, the large non-saturating magnetoresistance effect in semi-metals is easily utilized in the measurement of magnetic fields. For example, Fukuroi and Fukase (1964) have employed a magnetoresistance probe of antimony, showing a resistance change of 100:1 in a field of 10 koe at liquid helium temperature, in their studies of type II superconductivity. Bismuth is particularly useful for making magnetoresistance probes since it can be obtained in the form of thin ductile wires. Unfortunately, although the low-temperature magnetoresistance of bismuth is very large, it is rather sensitive to strain, and consistent behaviour from bismuth probes is difficult to achieve.

The non-linear effects observed, particularly for bismuth, at low temperatures suggest a number of possibilities. For example, Esaki (1962 b) has proposed that his kink effect could be used in the generation and detection of electromagnetic waves up to microwave frequencies, but the need for liquid helium temperature must make the alternative means of achieving the same result more practicable. The observation of sound amplification in bismuth by Toxen and Tansal (1963) which has already been mentioned, could, in principle, lead to the use of semi-metals in lossless (or amplifying) ultrasonic delay lines but the conditions seem more favourable for the wide-gap semiconductors, such as CdS, in which the power dissipation is low due to the very small carrier concentrations. The semi-metals need both a relatively high magnetic field and a low temperature.

The most important potential applications lie in the field of direct energy conversion. Bi₂Te₃ and its solid solutions with Sb₂Te₃ and Bi₂Se₃ are already widely used in thermoelectric refrigeration. The coefficient of performance for a thermocouple used as a refrigerator (or its efficiency if it is used as a generator) depends on the so-called figure of merit Z defined as $\alpha^2\sigma/\kappa$ (Ioffe 1957). Z reaches its largest values for semiconductors which have a favourable combination of carrier mobility, density-of-states effective mass and lattice thermal conductivity; the quantity $\mu(m^*/m)^{3/2}/\kappa_{\rm L}$ is a guide to the value of a specific material for thermoelectric applications. It is also desirable that the energy gap should be large enough for a reasonably high Seebeck coefficient (say 200–250 $\mu v/\deg$) to be obtained. This condition is normally satisfied if the energy gap exceeds about 5kT.

It has been shown by O'Brien and Wallace (1958) that the phenomenological relations for thermomagnetic energy conversion (utilizing the Nernst or Ettingshausen effects) are similar to those for thermoelectric energy conversion. In consequence, the thermomagnetic figure of merit $Z_{\rm NE}$ as defined in eqn. (37), has the same significance as the thermoelectric figure of merit. Delves (1962) first showed that the value of $Z_{\rm NE}$ for certain semi-metals might be appreciably larger than the highest known values of Z for semiconductors. This possibility arises from the high Nernst and Ettingshausen coefficients in intrinsic conductors; the electrons and holes transport their energy while sharing a common crystal lattice, whereas in a thermocouple two different materials (one n-type and one p-type) are needed and the lattice heat conduction is twice as great.

There are also advantages accruing from the application of a strong magnetic field, which reduces the electronic contribution to the thermal conductivity, while usually raising the average energy transported by a

charge carrier. These advantages can, however, sometimes be found for thermoelectric devices in a magnetic field. In fact, Simon (1964) has demonstrated the very close relationship between the thermomagnetic figure of merit of an intrinsic conductor and the thermoelectric figure of merit of a nearly-intrinsic conductor when both are placed in a strong magnetic field.

There have already been some notable advances towards useful Ettingshausen refrigeration. For example, Kooi et al. (1963) have obtained a cooling effect at 36 $^{\circ}$ K from a sink temperature of 156 $^{\circ}$ K using a rectangular sample of Bi₉₇Sb₃ in a field of 15 koe, while Harman et al. (1964) have been able to cool one face of a specially shaped bismuth sample by 101°k, the opposite face being kept at room temperature. Unfortunately this last experiment depended on the application of a field of 110 koe.

The electron parameters in bismuth and its alloys with antimony are adequate for thermomagnetic refrigeration but the performance is limited by the relatively low hole mobility. The fact that a really useful device could be made from a conductor with high hole and electron mobilities. a low lattice thermal conductivity and a close-to-zero energy gap must surely provide a stimulus to work on the transport properties of semi-metals and on widening the range of materials that is available for study.

References

ABELES, B., and MEIBOOM, S., 1956, Phys. Rev., 101, 544.

AIRAPETYANTS, S. V., and SHMELEV, G. I., 1960, Soviet Phys.—Solid State, 2, 689. Aubrey, J. E., James, C., and Parrott, J. E., 1964, Proc. Int. Conf. Semiconductor Phys., Paris, p. 689.

Austin, I. G., 1958, Proc. phys. Soc. Lond., 72, 545.

Austin, I. G., and Sheard, A. R., 1957, J. Electron. Contr., 3, 236.

BARDEEN, J., COOPER, L. N., and Schrieffer, J. R., 1957, Phys. Rev., 108,

BARRETT, C. S., CUCKA, P., and HAEFNER, K., 1963, Acta Cryst., 16, 451.

Beer, A. C., 1963, Galvanomagnetic Effects in Semiconductors (New York: Academic Press).

BIERLY, T. N., MULDAWER, L., and BECKMAN, O., 1963, Acta Met., 11, 447.

Bowley, A. E., Delves, R., and Goldsmid, H. J., 1958, Proc. phys. Soc., Lond., 72, 401.

BOYLE, W. S., and SMITH, G. E., 1963, Progr. in Semiconductors, 7, 1.

Brooks, H., 1955, Advan. electron. electron Phys., 7, 156.

Brown, D. M., and Heumann, F. K., 1964, J. appl. Phys., 35, 1947.

Brown, A., and Lewis, B., 1962, J. Phys. Chem. Solids, 23, 1597.

Brown, D. M., and Silverman, S. J., 1964, I.B.M. J., 8, 253.

Buckel, W., 1959, Z. Phys., 154, 474.

Busch, G. A., and Kern, R., 1960, Solid State Phys., 11, 1.

Busch, G. A., Steigmeier, E., and Wettstein, E., 1959, Helv. phys. Acta,

Busch, G. A., and Wieland, J., 1953, Helv. phys. Acta, 26, 697.

CARDONA, M., PAUL, W., and BROOKS, H., 1960, Helv. phys. Acta, 33, 329.

Chapnik, I. M., 1962, Soviet Phys.—Dokl., 6, 988.

COHEN, M. H., 1961, Phys. Rev., 121, 387.

COHEN, M. H., FALICOV, L. M., and GOLIN, S., 1964, I.B.M. J., 8, 215.

COHEN, M. L., 1964, Phys. Rev., 134, A511.

CONWELL, E. M., and WEISSKOPF, V. F., 1950, Phys. Rev., 77, 388.

CUCKA, P., and BARRETT, C. S., 1962, Acta Cryst., 15, 865.

DATARS, W. R., and DEXTER, R. N., 1961, Phys. Rev., 124, 75.

DATARS, W. R., and VANDERKOOY, J., 1964, I.B.M. J., 8, 247.

Delves, R. T., 1962, Brit. J. appl. Phys., 13, 440; 1964, Ibid., 15, 105.

Delves, R. T., Bowley, A. E., Hazelden, D. W., and Goldsmid, H. J., 1961, Proc. phys. Soc., Lond., 78, 838.

Drabble, J. R., 1958, Proc. phys. Soc., Lond., 72, 380; 1963, Progr. in Semiconductors, 7, 47.

DRABBLE, J. R., and Goldsmid, H. J., 1961, Thermal Conduction in Semiconductors (Oxford: Pergamon Press).

DRABBLE, J. R., and GOODMAN, C. H. L., 1958, J. Phys. Chem. Solids, 23, 1597. DRABBLE, J. R., GROVES, R. D., and WOLFE, R., 1958, Proc. phys. Soc., Lond.,

71, 430.

Drabble J. R., and Wolfe, R., 1956, Proc. phys. Soc. Lond. B 69, 1101.

DRABBLE, J. R., and Wolfe, R., 1956, Proc. phys. Soc., Lond., B, 69, 1101; 1957, J. Electron. Contr., 3, 259.

EASTMAN, P. C., and DATARS, W. R., 1963, Canad. J. Phys., 41, 161.

EFIMOVA, B. A., KORENBLIT, I. Y., NOVIKOV, V. I., and OSTROUMOV, A. G., 1962, Soviet Phys.—Solid State, 3, 2004.

EHRENREICH, H., 1961, J. appl. Phys., 32, 2155.

EPSTEIN, S., and JURETSCHKE, H. J., 1963, Phys. Rev., 129, 1148.

ERTL, M. E., PFISTER, G. R., and GOLDSMID, H. J., 1963, Brit. J. appl. Phys., 14, 161.

ESAKI, L., 1962 a, *Phys. Rev. Letters*, **8**, 4; 1962 b, *Proc. Inst. Radio Engrs*, NY., **50**, 322.

Esaki, L., and Stiles, P. J., 1965, Phys. Rev. Letters, 14, 902.

Falicov, L. M., and Golin, S., 1965, Phys. Rev., 137, A871.

Freedman, S. J., and Juretschke, H. J., 1961, Phys. Rev., 124, 1379.

FRIEDMAN, A. N., and Koenig, S. H., 1960, I.B.M. J., 4, 158.

Fröhlich, H., and Kittel, C., 1954, Physica, 20, 1086.

Fukuroi, T., and Fukase, T., 1964, Sci. Rep. Res. Inst. Tohoku Univ., A, 16, 132.

Gallo, L. F., Chandrasekhar, B. S., and Sutter, P. H., 1963, *J. appl. Phys.*, **34**, 144.

GALLO, C. F., MILLER, R. C., SUTTER, P. H., and URE, R. W., 1962, J. appl. Phys., 33, 3144.

Goldsmid, H. J., 1956, Proc. phys. Soc. Lond., B, 69, 203; 1962, GEC J., 29, 158.

Goldsmid, H. J., and Corsan, J. M., 1964, Phys. Letters, 8, 221.

GOODMAN, C. H. L., 1958, J. Phys. Chem. Solids, 6, 305.

Goss, A. J., and Weintroub, S., 1952, Proc. phys. Soc., Lond., B, 65, 561.

Gurevich, L., 1945, J. Phys. U.S.S.R., 9, 477.

HALL, J. J., and Koenig, S. H., 1964, I.B.M. J., 8, 241.

Hannay, N. B., Geballe, T. H., Matthias, B. T., Andres, K., Schmidt, P., and MacNair, D., 1965, Phys. Rev. Letters, 14, 225.

HARMAN, T. C., 1961, J. appl. Phys., 32, 1800.

HARMAN, T. C., HONIG, J. M., FISCHLER, S., PALADINO, A. E., and BUTTON, M. J., 1964, Appl. Phys. Letters, 4, 77.

Hashimoto, K., 1961, J. phys. Soc., Japan, 16, 1970.

HATTORI, T., and STEELE, M. C., 1963, J. phys. Soc., Japan, 18, 1294.

HATTORI, T., and Tosima, S., 1965, J. phys. Soc., Japan, 20, 44.

Hein, R. A., Gibson, J. W., Mazelsky, R., Miller, R. C., and Hulm, J. K., 1964, Phys. Rev. Letters, 12, 320.

HERRING, C., 1958, Semiconductors and Phosphors, Ed. M. Schon and H. Welker (New York: Interscience), p. 184.

HOPFIELD, J. J., 1962, Phys. Rev. Letters, 8, 311.

HURLE, D. T. J., 1963, Prog. in Materials Science, 10, 79.

HUTSON, A. R., McFee, J. H., and White, D. L., 1961, Phys. Rev. Letters, 7, 237.

IOFFE, A. F., 1957, Semiconductor Thermoelements and Thermoelectric Cooling (London: Infosearch).

JAIN, A. L., 1959, Phys. Rev., 114, 1518.

JAIN, A. L., and KOENIG, S. H., 1962, Phys. Rev., 127, 442.

KLEIN, C. A., 1964, J. appl. Phys., 35, 2947.

KLEIN, C. A., and HOLLAND, M. G., 1963, Bull. Amer. phys. Soc., 8, 208.

KLEIN, C. A., STRAUB, W. D., and DIEFENDORF, R. J., 1962, Phys. Rev., 125, 468.

KOOI, C. F., HORST, R. B., CUFF, K. F., and HAWKINS, S. R., 1963, J. appl. Phys., 34, 1735.

LANDWEHR, G., and DRATH, P., 1964, Proc. Int. Conf. Semiconductor Phys., Paris, p. 670.

Lange, P. W., 1939, Naturwissenschaften, 27, 133.

Lax, B., Mayroides, J. G., Zeiger, H. J., and Keyes, R. J., 1960, Phys. Rev. Letters, 5, 241.

LERNER, L. S., 1962, Phys. Rev., 127, 1480; 1963, Ibid., 130, 605.

McClure, J. W., 1964, I.B.M. J., 8, 255.

MISRA, S., and BEVER, M. B., 1964, J. Phys. Chem. Solids, 25, 1233.

Moriguchi, Y., and Koga, Y., 1957, J. phys. Soc., Japan, 12, 100.

O'BRIEN, B. J., and WALLACE, C. S., 1958, J. appl. Phys., 29, 1010.

PAUL, W., 1961, J. appl. Phys., 32, 2082.

PIPPARD, A. B., 1963, Phil. Mag., 8, 161.

PORBANSKY, E. M., 1959, J. appl. Phys., 30, 1455.

PRICE, P. J., 1960, I.B.M. J., 4, 152.

RODOT, M., RODOT, H., and TRIBOULET, R., 1961, J. appl. Phys., 32, 2254.

Rosi, F. D., Hockings, E. F., and Lindenblad, N. E., 1961, R.C.A. Rev., 22, 82.

SAUNDERS, G. A., COOPER, G., MIZIUMSKI, C., and LAWSON, A. W., 1965, J. Phys. Chem. Solids, 26, 533.

SAUNDERS, G. A., and LAWSON, A. W., 1965, J. appl. Phys., 36, 1787.

SEHR, R., and TESTARDI, L. R., 1963, J. appl. Phys., 34, 2754.

Shoenberg, D., 1938, Superconductivity (Cambridge: University Press).

SIMON, R., 1964, Advanced Energy Conversion, 4, 237.

SMITH, G. E., 1962, Phys. Rev. Letters, 9, 487.

SMITH, G. E., BARAFF, G. A., and ROWELL, J. M., 1964, I.B.M. J., 8, 228.

SMITH, G. E., WOLFE, R., and HASZKO, S. E., 1964, Proc. Inst. Conf. Semiconductor Phys., Paris, p. 399.

Soule, D. E., 1958, Phys. Rev., 112, 698.

Suzuki, M., Kikuchi, S., and Hatoyama, G. M., 1964, Proc. Int. Conf. Semi-conductor Phys., Paris, p. 647.

TESTARDI, L. R., STILES, P. J., and BURSTEIN, E., 1962, Bull. Amer. phys. Soc., 7. 548.

Tosima, S., and Hattori, T., 1964, J. phys. Soc., Japan, 19, 2022.

TOXEN, A. M., and TANSAL, S., 1963, Phys. Rev. Letters, 10, 481.

TSIDIL'KOVSKII, I. M., 1962, Thermomagnetic Effects in Semiconductors (London: Infosearch).

Turner, W. J., Fischler, A. S., and Reese, W. E., 1961, J. appl. Phys., 32, 2241.

URE, R. W., 1962, Proc. Int. Conf. Semiconductor Phys., Exeter, p. 659.

VAN LEUT, P. H., 1962, Acta Met., 10, 1089.

Vuillemin, J., 1964, I.B.M.J., **8,** 232.

326 On Transport Effects in Semi-metals and Narrow-gap Semiconductors

WHITSETT, C. R., 1961, J. appl. Phys., 32, 2257.

WILSON, A. H., 1953, The Theory of Metals, 2nd edition (Cambridge: University Press).

Wolfe, R., and Smith, G. E., 1962, Proc. Int. Conf. Semiconductor Phys., Exeter, p. 771. WRIGHT, D. A. 1959, Electron. Engng, 31, 659.

Wyckoff, R. W. G., 1960, Crystal Structures, 1 (New York: Interscience). ZITTER, R. N., 1962, Phys. Rev., 127, 1471; 1965, Phys. Rev. Letters, 14, 14.